

*C 12 86229*  
N 69 . 3 6 9 8 3

NASA CR 86229

7496-362

RESEARCH TO DETERMINE CLOUD  
AND SYNOPTIC PARAMETERS  
ASSOCIATED WITH CLEAR AIR TURBULENCE

(INTERIM REPORT)

by Duane S. Cooley and John T. Ball

July 1969

CASE FILE  
COPY

Distribution of this report is provided in the interest of information exchange and should not be construed as endorsement by NASA of the material presented. Responsibility for the contents resides in the organization that prepared it.

Prepared under Contract No. NAS12-699 by  
THE TRAVELERS RESEARCH CORPORATION  
250 Constitution Plaza      Hartford, Connecticut 06103

Electronics Research Center  
NATIONAL AERONAUTICS AND SPACE ADMINISTRATION

RESEARCH TO DETERMINE CLOUD  
AND SYNOPTIC PARAMETERS  
ASSOCIATED WITH CLEAR AIR TURBULENCE  
  
(INTERIM REPORT)

by Duane S. Cooley and John T. Ball

July 1969

Prepared under Contract No. NAS12-699 by  
THE TRAVELERS RESEARCH CORPORATION  
250 Constitution Plaza      Hartford, Connecticut 06103

Electronics Research Center  
NATIONAL AERONAUTICS AND SPACE ADMINISTRATION

## FOREWORD

The Electronics Research Center Technical Monitor is:

Mr. George Economou  
Code PH  
NASA Electronics Research Center  
565 Technology Square  
Cambridge Massachusetts 02139



## ABSTRACT

The objective of this research is to deduce and study relationships between clear air turbulence (CAT) in the stratosphere and upper troposphere with meteorological variables, circulation data and cloud features. The principal turbulence data used were instrumented reports of CAT in the 45,000- to 70,000-ft layer obtained by the U.S. Air Force in Project HICAT during 1966 and 1967.

Approximate quantitative specifications were determined for ranges of parameters representing vertical variation of wind and temperature derived from rawinsonde observations. Large values of wind shear and negative values of temperature lapse rate or irregular lapse rate in the stratosphere were often associated with at least light to moderate intensity of CAT. Significant stratospheric CAT appears also to be associated with strong southwesterly flow and with banded and cumulonimbus clouds.



## ACKNOWLEDGEMENTS

Our sincere thanks go to Mr. G. Economou of NASA/Electronics Research Center for his help, interest and cooperation during the course of this study.

The turbulence, satellite and meteorological data used were due to the efforts of many individuals and organizations. The published Project HICAT data prepared by Lockheed-California Company under contract to Air Force Flight Dynamics Laboratory, Wright-Patterson Air Force Base, Ohio provided the basis for stratospheric CAT analyses. Commercial and military reports in the upper troposphere were generously provided by Mr. DeVer Colson of the Weather Bureau, ESSA. Satellite picture mosaics and film were provided by the National Environmental Satellite Center, ESSA and National Weather Records Center, ESSA. Satellite infrared data were furnished by the National Space Science Data Center through the assistance of the Wolf Research and Development Corporation. Surface and upper level charts routinely published by the Free University of Berlin were utilized in determining concurrent circulation features.

Several individuals at The Travelers Research Corporation made many notable contributions. Mr. Frank Perry with the guidance of Mr. Marshall Atwater wrote the program to compute meteorological variables from radiosonde and rawinsonde measurements. Considerable data preparation and analysis were expertly accomplished by Mr. Charles Mulé.





## TABLE OF CONTENTS

<u>Section</u>	<u>Title</u>	<u>Page</u>
1.	INTRODUCTION	1
2.	DATA SOURCES	5
3.	ANALYSIS AND RESULTS	11
A.	Meteorological Variables	13
Symbols		16
Case Studies		25
Summary of CAT Relationships with Meteorological Variables		38
B.	Satellite Television and Infrared Data	40
C.	Atmospheric Circulation Features	48
4.	LOCATING PROBABLE REGIONS OF CLEAR AIR TURBULENCE	55
5.	SUMMARY	61
6.	REFERENCES	63
APPENDIXES		
A.	COMPUTER PROGRAM SPECIFICATIONS	65

## LIST OF TABLES

<u>Table</u>	<u>Title</u>	<u>Page</u>
2-1	Selected HICAT phase 2 sample dates	7
3-1	Average value of meteorological variable for indicated turbulence intensity category	14
3-2	Average values of meteorological variables for combined turbulence intensity categories	15
3-3	Average values of meteorological variables associated with CAT in the upper troposphere	21
3-4	Contingency table comparison of meteorological variables and clear air turbulence	23
3-5	Contingency table comparison of joint variables and clear air turbulence	27

<u>Table</u>	<u>Title</u>	<u>Page</u>
3-6	Major television features of HICAT observations frequency summarized by cloud category	44
3-7	Observations (from ESSA) over or near major satellite television cloud features	46
3-8	Percent frequency distributions of circulation features stratified according to CAT intensity	49

### LIST OF ILLUSTRATIONS

<u>Figure</u>	<u>Title</u>	<u>Page</u>
3-1	Graph of $\bar{V} \cdot \frac{\Delta \bar{V}}{\Delta Z} \times \gamma_{\min}$ for determining CAT likelihood	26
3-2	Graph of $\bar{V} \cdot \frac{\Delta \bar{V}}{\Delta Z} \times \gamma_{\max}$ for determining CAT likelihood	26
3-3	HICAT research flight T-54 on April 1, 1966 from 1825 - 2225 GMT[ 9]	28
3-4(a)	Sounding at Las Vegas, Nevada on April 2, 1966 at 0000 GMT	32
3-4(b)	Sounding at Boise, Idaho on Aug. 25, 1966 at 0000 GMT	32
3-5(a)	Sounding at Hilo, Hawaii on May 14, 1966 at 0000 GMT	35
3-5(b)	Sounding at Lihue, Hawaii on May 14, 1966 at 0000 GMT	35
3-6(a)	Sounding at Portland, Maine on September 30, 1966 at 1200 GMT	37
3-6(b)	Sounding at Albany, N. Y. on September 30, 1966 at 1200 GMT	37
3-7	Idealized characteristics of satellite video data	41
3-8	ESSA 3 picture on Jan 4, 1967 (2028 GMT) showing small wave clouds at 39°N, 116° to 118° W, nearly transverse to the 400 mb wind of 267°, 102 ft sec <sup>-1</sup> measured at Ely, Nevada (0000 GMT, Jan 5, 1967) about 150 miles to the east	43

## 1. INTRODUCTION

The objectives of the research described in this report are to study cloud and synoptic parameters associated with clear air turbulence (CAT) in the stratosphere and upper troposphere, to determine relationships between CAT and these parameters, and to develop a model or set of procedures for the prediction of turbulence occurrence. The research is specifically directed toward the ultimate delineation of those atmospheric parameters most associated with CAT occurrence for subsequent design of detection instrumentation.

Turbulence in the atmosphere, in general, refers to the instantaneous departure of the wind flow from a time-averaged mean. In CAT research, we are specifically concerned with those fluctuations or "eddies" in the wind flow that have a scale dimension (approximately 50—500 feet) to which aircraft are responsive. Aircraft response is felt as a series of vertical accelerations or "bumps" that cannot ordinarily be compensated by the pilot. CAT in the upper troposphere and lower stratosphere includes turbulence encountered by aircraft both in clear air (clouds may be present below or above the aircraft level) and in or close to cirrus clouds. Turbulence and large updrafts encountered in and very near convective clouds are considered a separate problem.

A list of previous CAT research is provided in the references section and will not be given in detail in this report. The reader is referred particularly to an assessment by the National Committee for Clear Air Turbulence [1] and a summary of papers given at the most recent Symposium on Clear Air Turbulence and Its Detection [2]. As background for detailed evaluation of the results of this study a summary of previous studies is provided.

Clodman, Morgan and Ball [3] proposed two basic mechanisms associated with the presence of gravity waves and strong vertical wind shear, and dynamic instability (strong anticyclonic wind shear and curvature) and a low Richardson number. Reiter and Nania [4] have noted the occurrence of clear air turbulence in thermally stable layers of the atmosphere in which the wind is turning with height and also suggest a gravity-wave mechanism. In relatively thin layers in which the vertical wind shear is strong, the large scale wind flow can become disorganized, thus resulting in the transfer of energy to higher wave numbers and into small scale turbulence [5].

Numerous studies during the 1950's and 1960's have associated turbulence in the mid- and upper troposphere and lower stratosphere with such synoptic features as upper-level troughs and lows, the jet-stream and tropopause, upper level fronts and thermal ribbons [6] and meteorological variables measured on a synoptic scale. The variance of results is not surprising considering the differing characteristics of the data samples. Some meteorological variables correlated with turbulence are: wind speed, vertical and horizontal wind shear, temperature lapse rate, horizontal temperature gradient, differential temperature advection, Richardson Number, and other derived quantities such as the divergence and vorticity of the wind and the product of wind speed and turning of the wind with height [7] .

It should be noted that all synoptic studies reflect indirect statistical relationships since turbulence which is a micro-scale phenomenon is being related to atmospheric flow and stability observed on a synoptic scale (100 to 1000 mi). When subjective (non-instrumented) reports of turbulence constitute the sample being analyzed, the difficulties in establishing strong relationships are obvious.

Some stratospheric CAT sampling programs suggest that CAT tends to decrease in both frequency and intensity with altitude above 40,000 feet. However, moderate to severe turbulence has been experienced at altitudes up to 70,000 feet by such aircraft as U-2, Canberra, B-70 and SR71 [8] . An analysis of HICAT data by Crooks, et al. [9] reveals that the median dimensions of stratospheric CAT areas below 70,000 feet seem to be of the order of 15 miles in the horizontal and 2000 feet in the vertical. The dimensions of turbulence patches in the troposphere are similar in vertical extent but have average horizontal dimensions of about 50 miles [10] . In all discussions of variations of turbulence characteristics with altitude, one must be aware of the differences in type (subjective or instrumented), quality, and quantity of input turbulence data. Furthermore, considerations must be also given to such factors as location, season and time of day. The current status and problems in CAT research can be summarized as:

CAT in the troposphere appears to be associated with meso-scale motions of the wind field which become disorganized in thin layers of strong vertical wind shear and a major problem is the

difficulty of relating this micro- or meso-scale phenomenon to synoptic scale variables.

Statistical summaries of frequency and intensity of stratospheric CAT have been made from instrumented aircraft flights. The relative importance of upper tropospheric disturbances to CAT in the stratosphere has not been clearly determined.

CAT in the upper troposphere has been related to the season of the year, underlying terrain and certain meteorological features of a synoptic scale.

Research efforts have been frequently restricted in the past by the use of subjective pilot reports of CAT where problems of interpretation by the pilot are compounded by the fact that different types of aircraft vary in response characteristics.

Satellite pictures depict cloud features associated with both synoptic-scale and meso-scale circulation features. The principal cloud features are: Size, shape and organization, orientation, texture, tone or brightness, presence of shadow and overall homogeneity. As an example, Viezee, et al. [11] studied four features of jet-stream cirrus clouds (shadow lines, sharp-edged cirrus sheets, cirrus bands and transverse waves) in relation to the observed wind field. Crooks, et al. [9] noted from aircraft cloud photographs that turbulence was found to occur above an abrupt edge or a large break in the cirrus deck, high lenticular cirrus clouds, the tops of cumulonimbus clouds and cirrus streaks or wisps and long streaming cumulonimbus anvils. Usually these features can be identified in satellite photographs having good resolution. In this investigation satellite video data were studied for the information that can be determined regarding both synoptic and meso-scale circulation features related to CAT occurrence. We were concerned with determining the importance, of upward propagations from upper tropospheric levels as revealed by these video data.

The ALLCAT program [12] in general and, specifically, the HICAT flight data presented an opportunity to examine a significant volume of instrumented turbulence data which permit an examination and assessment of the applicability of tropospheric

turbulence theory to CAT in the stratosphere. In addition to these HICAT data other data utilized in this study include satellite video and infrared data, commercial aircraft reports of turbulence, meteorological vertical soundings of temperature and winds, and constant pressure surface analyses. These data sources are described in Section 2. The detailed technical analyses of data are presented in Section 3. A procedure for locating probable CAT regions in the stratosphere is discussed and evaluated in Section 4. Finally, Section 5 summarizes the results of the study including delineation of those features likely to be associated with clear air turbulence.

## 2. DATA SOURCES

The principal source of turbulence data was instrumented reports of CAT in the stratosphere collected by the U.S. Air Force in the HICAT portion of their ALLCAT program [13]. These data are published in three volumes [9] containing flights between October 1965 and February 1967 (Phase 2) and in two volumes [14] for the period March 1967 through February 1968 (Phase 3). These include a flight description and flight track maps, total hours flown and time flown in CAT, horizontal and vertical locations and intensity of turbulence regions, and radiosonde data from 150 mb to 50-mb constant pressure surfaces including significant temperature levels. For portions of many flights, gust velocity time histories and power spectra of vertical, longitudinal and lateral gust velocities are included. The flight data were collected at altitudes from 45,000 to 70,000 feet over various locations in and near the contiguous United States, Hawaii, Alaska, Australia, New Zealand, England and Panama. In the Phase 2 program, 29.2 hours of CAT were encountered over flights covering 256,000 miles (649.5 flight hours). In the Phase 3 portion, 18.3 hours of CAT were recorded over 156,000 miles (477.6 flight hours). In the original editing of the data, the intensity of CAT was classified according to the estimated level of the center of gravity (cg) acceleration peaks as follows [9]:

<u>CAT category</u>	<u>Frequently occurring peak g increment</u>
Very light (VL)	$\pm 0.05$ to $\pm 0.10$
Light (L)	$\pm 0.10$ to $\pm 0.25$
Moderate (M)	$\pm 0.25$ to $\pm 0.50$
Severe (S)	$\pm 0.50$ to $\pm 0.75$
Extreme (X)	$\pm 0.75$ or greater

Other intensity classifications used are light to moderate (LM) and moderate to severe (MS). Occasional cg accelerations of  $\pm 0.25$  to  $\pm 0.50$  result in an LM classification and similarly, occasional peaks  $\pm 0.50$  to  $\pm 0.75$  dictate a MS classification. Subjective pilot reports were utilized in this study to define cases of more intense CAT ( $\geq$  LM) in only a few instances and were primarily employed to corroborate that no turbulence or only very light or light CAT were encountered.

Phase 2 HICAT data constitute the basic turbulence data used in this particular study but also a limited portion of the Phase 3 data were included for preliminary verification. Continuing studies are currently underway using most Phase 3 measurements. Table 2-1 lists the dates from the HICAT Phase 2 sample used in this study. Other information included in the table is the location, total number of cases, number of cases of light to moderate or greater CAT and whether the date was included in the satellite portion of the study. Data from the flights based in Australia and New Zealand were not included. Only limited use was made of the flight data over Alaska because background illumination in February 1967 precluded obtaining useful ESSA 2 pictures. Essentially all other cases of light to moderate or more intense CAT measured in the HICAT Phase 2 program were included regardless of the quality of the satellite picture data.

A second source of data was a compilation of collected military and commercial subjective pilot reports of CAT primarily in the 30,000- to 40,000-foot layer for the period January—June 1966. These include time, location, altitude, estimate of intensity, type of aircraft and occasionally temperature and wind data. This sample does not contain reports of non-occurrences of CAT or of CAT with a subjective intensity less than light to moderate. By definition, a case of CAT consisted of the most representative intensity of 3 to 5 or more subjective reports. A total of 47 cases were selected with 22 characterized by light to moderate intensity, 22 as moderate CAT, and 3 as moderate to severe CAT. Table 2-2 gives the dates and number of cases.

The meteorological variables were computed from standard rawinsonde soundings taken twice-daily at 0000 and 1200 GMT. Tabulations of wind direction and speed at mandatory constant pressure levels (150, 100, 70 and 50 mb) and temperatures at these levels and at significant levels were listed in volume III of the Project HICAT publication [9]. These data were supplemented by height, temperature, and wind data at intervening standard pressure levels (125, 80 and 60 mb) which were extracted from Northern Hemisphere Data Tabulation on microfilm. Additionally, sounding data from 400 to 150 mb were tabulated. However, detailed and small scale variations of the temperature and wind fields in the vertical are not provided. This is particularly true of the wind field, where sounding data such as that obtained by the Jimsphere balloon is required for the determination of vertical wind shear over a thin layer. However,



TABLE 2-1  
SELECTED HICAT PHASE 2 SAMPLE DATES

Date	Location	Reports of light to moderate or greater CAT	Photo coverage
1965 Nov 17 1966 Mar 22 Mar 25 Mar 28 Mar 31 Apr 1 Apr 5 Apr 6	Western United States	yes no no no yes yes no no	no yes yes yes yes yes yes yes
1966 Apr 18 Apr 20 Apr 21 Apr 22 Apr 25 Apr 26 Apr 27 Apr 29 May 2 May 5 May 10 May 13 May 16 May 17 May 19 May 20	Pacific Ocean	no yes no no yes no no yes yes no no yes yes yes no yes yes	yes no yes no no yes yes no no yes yes yes yes no yes no
1966 Aug 24 Aug 29 Aug 30 Aug 31	Western United States	no yes yes no	yes yes* no yes
1966 Sep 21 Sep 28 Sep 29 Sep 30 Oct 18 Oct 20 Oct 21 Oct 24	Eastern United States	yes no no yes no yes no yes	yes yes* yes* yes* yes* yes yes yes*

\*HRIR data used.

Table 2-1 (Continued)

Date	Location	Reports of light to moderate or greater CAT	Photo coverage
1966 Oct 25 Oct 26 Oct 27 Oct 28		no no no yes	yes yes* yes* yes
1966 Nov 4 Nov 7 Nov 9 Nov 10 Nov 14 Nov 15 Nov 16 Nov 17 Nov 21 Nov 23	Caribbean	yes yes no yes no no yes no no no	yes* no yes yes yes yes yes yes yes yes
1967 Jan 1	Western U.S.	yes	yes
1967 Jan 16 Feb 6	Alaska	yes yes	no no

Total cases: 176

Total photo cases: 90

Total cases of light to moderate or greater CAT: 40

\*HRIR data used.

TABLE 2-2

SUBJECTIVE CASES OF LIGHT TO MODERATE OR MORE INTENSE  
CAT IN THE UNITED STATES

Date	Cases	Date	Cases	Date	Cases
1966 Feb 11	3	1966 Mar 31	1	1966 May 10	2
Feb 12	3	Apr 2	1	May 11	2
Feb 15	5	Apr 3	3	May 16	2
Feb 16	2	Apr 18	1	May 20	1
Mar 17	5	Apr 19	4	Jun 9	1
Mar 18	3	Apr 25	2	Jun 19	1
Mar 22	5	Apr 25	2	Jun 10	1

with a sufficiently large sample, the routine sounding data can be effectively utilized in examining the relationship of atmospheric conditions to CAT occurrence. Perhaps the most important problem is the higher frequency of missing wind data in the stratosphere during conditions of strong wind flow and increased likelihood of significance (light to moderate or greater intensity) CAT. This difficulty was not of sufficient magnitude to prevent the determination of significant relationships with CAT as discussed in Section 3(A).

Weather satellite pictures used in this study were acquired from ESSA 1, ESSA 2, ESSA 3 and ESSA 5. Those from the latter satellite were used only in the evaluation. Pictures from the Automatic Picture Transmission cameras [15] aboard ESSA 2 were prepared in the form of mosaics on 20 × 24 in. photographic paper by the National Environmental Satellite Center (NESC) of ESSA. Individual pictures used in composing these mosaics were received on facsimile recorders. Pictures from the other satellites were received at The Travelers Research Corporation on 35 mm microfilm from the National Weather Records Center (NWRC) of ESSA.

These satellites provide at the earth's surface a best horizontal resolution of about two or three miles. This resolution is usually adequate to distinguish the general type of larger cloud masses (stratiform, cumuliform, or cirriform). Small cumulus and thin cirrus are frequently indistinguishable and this could be crucial missing data in some stratospheric turbulence cases.

Most of the HICAT observations were made within a few hours of the time when satellite pictures were taken. Nimbus II High Resolution Infrared (HRIR) observations on the other hand were made about ten hours earlier. On 9 days (26 cases) concurrent HRIR data and HICAT observations were available. The Nimbus II HRIR responds to radiation in the spectral region of 3.5–4.1 microns which is an atmospheric "window" [16]. The effective radiating temperature is nearly the earth's surface temperature in a clear sky area, or the cloud top temperature in a region of uniform overcast low or middle cloud. With broken skies the effective temperature is due to the radiation from a multiplicity of cloud top surfaces and internal cirrus cloud elements, as well as patches of land or water surface.

The circulation analyses used in the study were those published by the Free University of Berlin [17, 18] for the surface and the 300-mb and 100-mb constant pressure surfaces. The 300-mb level is representative of conditions in the upper troposphere at about 30,000-ft altitude. The 100-mb level is close to 53,000 ft and is representative of that portion of the stratosphere close to the levels of most of the HICAT flights (50,000–65,000 ft). These analyses are made over the entire Northern Hemisphere and are characteristically smooth, depicting large scale circulation features.

### 3. ANALYSIS AND RESULTS

From the basic HICAT Phase 2 data sample described in the previous section, 176 cases of turbulence and no turbulence were defined and associated with the closest radiosonde station. The identically defined cases were used in the association with circulation features, while a somewhat different procedure was required when analyzing the satellite data as is described in Section 3B.

Each case was defined from the following information:

- (1) flight track map of entire flight,
- (2) location on flight track of measured CAT "runs,"
- (3) summary of pilot evaluation of CAT intensities and locations, and
- (4) distribution of radiosonde stations.

A few simple rules or guidelines that were used are as follows:

- A portion of the flight track was considered non-turbulent if there were no processed turbulent "runs" and no indication of CAT by the pilot.
- Subjective reports of very light and light CAT by the pilot were accepted, if the information was precise, particularly with regard to location.
- Cases of light to moderate or more intense CAT were defined only from measured CAT except in three cases where particular circumstances warranted accepting the pilot report.
- Individual cases of CAT and no turbulence were required to be approximately 100 nautical miles apart or separated by at least 5000 ft in the vertical. There were only a few instances when more than one case of CAT was defined in the same region because of the vertical separation.
- When a series of turbulence runs was reported in one locality, the intensity chosen for the case reflected the most intense CAT measured in any of the runs.
- For some flights, a best estimate of the probable flight altitude had to be made for individual cases. This estimate was obtained from

recorded heights at locations of earlier or later turbulence runs and from pilot comments.

- Each defined case was associated with the closest reporting radiosonde station. Each available radiosonde sounding was associated with only one segment of flight location. Since the flights were frequently planned to pass close to radiosonde station locations, in only 31 of 176 cases did the separation exceed 100 nautical miles. In almost all cases the temporal separation was less than 6 hours and frequently was less than 3 hours.

## A. Meteorological Variables

Specifications for a computer program were written as part of the current research program to determine meteorological variables associated with clear air turbulence (CAT). The complete specification contained in Appendix A describes a program written for the IBM 360/40 computer.

The results presented in this section reflect the completion of the analysis of the relationships uncovered between the occurrence and non-occurrence of stratospheric CAT and meteorological variables computed from temperature and wind sounding data for Phase 2 HICAT data only. A description of the input data, procedures and variables computed for analysis is given in Appendix A.

The results presented naturally focus on those variables exhibiting the most promising relationships although some of the weaker relationships are also shown. Where appropriate, a statistical testing of the relative strengths of the relationships was made.

### Average Values for CAT Categories

Table 3-1 gives, for 16 variables, their average value for five categories of turbulence intensity. Due to missing data, the number of cases on which the averages are based, varies as follows:

<u>Category</u>	<u>Number of cases</u>
0 - no CAT	65 to 67
VL - very light CAT	26
L - light CAT	41 to 43
LM - light to moderate CAT	9 to 13
M - at least moderate CAT	24 to 27

The averages for the variables  $(\Delta \vec{V}/\Delta Z)_{\text{lower}}$  and  $|\Delta \gamma_L / \Delta Z|$  were based on fewer cases than the above. Since the number of cases in individual categories is not large, the none and very light categories were combined as were the light to moderate and moderate or greater categories. The averages computed for these combined categories are shown in Table 3-2.

TABLE 3-1  
AVERAGE VALUE OF METEOROLOGICAL VARIABLE FOR  
INDICATED TURBULENCE INTENSITY CATEGORY

Variable	Units	CAT Intensity				
		None	Very light	Light	Light—moderate	Moderate or greater
$\frac{\Delta \vec{V}}{\Delta Z}$	$\frac{\text{ft sec}^{-1}}{100 \text{ ft}}$	0.457	0.478	0.621	0.714	0.682
$ \gamma $	$\frac{^{\circ}\text{C}}{100 \text{ ft}}$	0.079	0.062	0.101	0.092	0.134
$\gamma$	$\frac{^{\circ}\text{C}}{100 \text{ ft}}$	0.060	0.040	0.054	0.028	0.101
Ri	—	107	145	45	13	85
Ri'	—	44	49	31	13	28
$\bar{V} \cdot \frac{\Delta \vec{V}}{\Delta Z}$	$\frac{\text{ft}^2 \text{ sec}^{-2}}{100 \text{ ft}}$	16.96	31.62	31.62	37.16	42.18
$\gamma_{\text{max}} - \gamma_{\text{min}}$	$\frac{^{\circ}\text{C}}{100 \text{ ft}}$	0.212	0.201	0.286	0.292	0.417
$\left(\frac{\Delta \vec{V}}{\Delta Z}\right)_{\text{max}}$	$\frac{\text{ft sec}^{-1}}{100 \text{ ft}}$	0.675	0.762	0.810	0.911	0.985
$WS_{\text{max}}$	$\text{ft sec}^{-1}$	98	148	128	128	135
$\gamma_{\text{max}}$	$\frac{^{\circ}\text{C}}{100 \text{ ft}}$	0.144	0.152	0.186	0.146	0.259
$\bar{V}$	$\text{ft sec}^{-1}$	36	56	56	59	62
$\gamma_{\text{min}}$	$\frac{^{\circ}\text{C}}{100 \text{ ft}}$	-0.067	-0.050	-0.101	-0.156	-0.157
$\left(\frac{\Delta \vec{V}}{\Delta Z}\right)_{\text{lower}}$	$\frac{\text{ft sec}^{-1}}{100 \text{ ft}}$	0.573	0.590	0.638	0.779	0.775
$\left(\bar{V} \cdot \frac{\Delta \vec{V}}{\Delta Z}\right)_{\text{max}}$	$\frac{\text{ft}^2 \text{ sec}^{-2}}{100 \text{ ft}}$	2.633	56.65	51.13	53.53	73.73
R'imi	—	36	38	25	13	10
$\left \frac{\Delta \gamma_L}{\Delta Z}\right $	$\frac{^{\circ}\text{C}(100 \text{ ft})^{-1}}{100 \text{ ft}}$	0.004	0.004	0.009	0.006	0.008



TABLE 3-2

AVERAGE VALUES OF METEOROLOGICAL VARIABLES FOR  
COMBINED TURBULENCE INTENSITY CATEGORIES

Variable	CAT Intensity		
	None and very light	Light	Light to moderate or greater
$\frac{\Delta \vec{V}}{\Delta Z}$	0.463	0.621	0.691
$ \gamma $	0.074	0.101	0.121
$\gamma$	0.054	0.054	0.077
Ri	118	45	66
Ri'	45	31	24
$\bar{V} \cdot \frac{\Delta \vec{V}}{\Delta Z}$	21.16	31.62	40.80
$\gamma_{\max} - \gamma_{\min}$	0.209	0.286	0.379
$(\frac{\Delta \vec{V}}{\Delta Z})_{\max}$	0.700	0.810	0.965
WS <sub>max</sub>	112	128	131
$\gamma_{\max}$	0.146	0.186	0.224
$\bar{V}$	43	56	62
$\gamma_{\min}$	-0.063	-0.101	-0.156
$(\frac{\Delta \vec{V}}{\Delta Z})_{\text{lower}}$	0.577	0.638	0.777
$(\bar{V} \cdot \frac{\Delta \vec{V}}{\Delta Z})_{\max}$	34.93	51.13	67.80
R'imi	37	25	11
$ \frac{\Delta \gamma_L}{\Delta Z} $	0.004	0.009	0.007

## Symbols

The variables given in the tables are listed and described below:

$\frac{\Delta \vec{V}}{\Delta Z}$  Vertical vector wind shear of the central layer. The central layer is defined as the layer that includes the reported occurrence or non-occurrence of turbulence. The layer is determined by the closest wind (temperature) data above and below the CAT occurrence level.

$|\gamma|$  Absolute value of the lapse rate of the central layer.

$\gamma$  Lapse rate of the central layer.

Ri Richardson Number of central layer.

Ri' Richardson Number of central layer. All values greater than 100 are set equal to 100.

$\bar{V} \cdot \frac{\Delta \vec{V}}{\Delta Z}$  Product of the mean wind speed and vertical vector shear of the central layer; in effect, the gradient of kinetic energy.

$\gamma_{\max} - \gamma_{\min}$  Difference between the maximum and minimum lapse rates within  $\pm 6500$  ft ( $\pm 2000$  m) of level of occurrence or non-occurrence of CAT.

$(\frac{\Delta \vec{V}}{\Delta Z})_{\max}$  Maximum vertical vector wind shear. The largest of the shears computed for a central layer or a layer above or below, provided the wind data is within  $\pm 6500$  ft of level of occurrence or non-occurrence of CAT.

WS<sub>max</sub> Maximum wind speed at any level.

$\gamma_{\max}$  Maximum lapse rate within  $\pm 6500$  ft of level of occurrence or non-occurrence.

$\bar{V}$  Mean wind speed of central layer

$\gamma_{\min}$  Minimum lapse rate within  $\pm 6500$  ft of level of occurrence or non-occurrence of CAT.

$(\frac{\Delta \vec{V}}{\Delta Z})_{\text{lower}}$  Vertical vector wind shear of layer below central layer.

$(\bar{V} \cdot \frac{\Delta \vec{V}}{\Delta Z})_{\max}$  Maximum gradient of kinetic energy within  $\pm 6500$  ft of level of occurrence.

R'imi Richardson Number based on minimum lapse rate within  $\pm 6500$  ft of level of occurrence.

$\left| \frac{\Delta \gamma_L}{\Delta Z} \right|$  Rate of change of lapse rate (see Appendix A for further details).

As indicated by the average values of the variables for the intensity categories shown in Tables 3-1 and 3-2, many of the parameters are clearly related to the occurrence of turbulence. As a starting point in the analysis let us briefly discuss and eliminate those variables not well related to CAT.

Lapse rate. At least, using the procedure of an arithmetic average, the lapse rate does not distinguish among the categories none through light to moderate. Consideration of the absolute value or of the maximum or minimum value in a layer is more useful. A measure of the rate of change of lapse rate  $\left| \Delta \gamma_L / \Delta Z \right|$  (see Appendix A) is also poorly related to CAT.

Richardson Number ( $Ri$  and  $Ri'$ ). A weak relationship is apparent when large values of  $Ri'$  are limited to 100 so as not to distort the averages. However, even for  $Ri'$  there is little difference in the averages computed for light and moderate CAT. The different scales for which temperature and wind data are determined has always complicated the computation of  $Ri$  from standard sounding data and rarely have strong relationships been demonstrated. More detailed wind profiles such as those obtained with the Jimsphere balloon allow a more meaningful computation of  $Ri$ .

Maximum wind speed  $(WS)_{\max}$  and mean wind speed of the central layer  $(\bar{V})$ . It is not too surprising that the maximum wind observed in the sounding (usually below the 42,000 ft level) is poorly correlated to CAT in the 45,000 to 75,000 ft levels. A wide variety of atmospheric conditions can be present in the stratosphere for both strong and weak upper topospheric flow, rendering a significant relationship unlikely. There is a slight indication of stronger wind speeds at the level of occurrence being related to more intense CAT, but the difference in averages computed for moderate and light CAT is very small ( $7 \text{ ft sec}^{-1}$ ).

The remaining ten variables in the two tables all exhibit recognizable and significant differences among the computed averages for most or all of the categories of CAT. Each of these variables related is discussed below.

(1) Vertical vector wind shear of central layer ( $\Delta \vec{V} / \Delta Z$ ). CAT in the upper troposphere has probably been more consistently associated with the vertical vector shear of the horizontal wind than any other single meteorological variable. However, it has been contended by Crooks, et al. [14] that "the wind observations available to the aviation meteorologist lack the resolution desired for accurate calculation of wind shears at the HICAT levels and are considered inadequate for use in the prediction of high altitude clear air turbulence." The wind data referenced was reported at mandatory levels (150 mb, 100 mb, 70 mb and 50 mb) and at 5000-ft intervals. The data we utilized were extracted from Northern Hemisphere Data Tabulations on microfilm and the winds were reported at standard levels (150 mb, 125 mb, 100 mb, 80 mb, 70 mb, 60 mb, and 50 mb). The height intervals between these constant pressure surfaces are approximately equivalent to or somewhat less than the 5000 ft intervals. We feel on the basis of results obtained from analyses in this study that the above statement may be too pessimistic. The average shear computed for the no turbulence cases is  $0.457 \text{ ft sec}^{-1}$  per 100 ft and this increases to  $0.682 \text{ ft sec}^{-1}$  per 100 ft for moderate CAT. The value of 0.714 for light to moderate CAT probably reflects the small number of cases in this category. The vertical vector wind shear of the lower layer  $(\frac{\Delta \vec{V}}{\Delta Z})_{\text{lower}}$  appears to be somewhat less well related, considering either the 3 or 5 category averages.

(2) Vertical gradient of kinetic energy ( $\bar{V} \cdot \frac{\Delta \vec{V}}{\Delta Z}$ ). Expressed in units of  $\text{ft}^2 \text{ sec}^{-2}$  per 100 ft, large vertical gradients of energy indicate a potential for considerable energy exchange in the vertical with consequent perturbations or fluctuations of the flow and CAT. The values of 37.16 and 42.18 for light to moderate and moderate CAT contrast with the average value of 16.96 computed for non-turbulence cases. The maximum gradient of kinetic energy  $(\bar{V} \cdot \frac{\Delta \vec{V}}{\Delta Z})_{\text{max}}$  is similarly related to CAT except that the average values are close to twice as large (see 3 category averages).

(3) Minimum lapse rate ( $\gamma_{\text{min}}$ ). The average value in  $^{\circ}\text{C}$  per 100 ft computed for light to moderate or greater CAT of  $-0.156$  contrasts with the average of  $-0.063$  computed for no CAT and very light CAT. A layer with a significant negative lapse rate in the stratosphere where the overall lapse rate is generally positive or nearly isothermal clearly contributes to an irregular temperature profile. Richardson

Number computed with this lapse rate ( $R'_{imi}$ ) has an average value of 37 for no turbulence and very light CAT and only 11 for light to moderate or greater CAT.

(4) The difference between the maximum and minimum lapse rates ( $\gamma_{\max} - \gamma_{\min}$ ), expressed in °C per 100 ft appears to discriminate well among the categories of none and very light, light, and light to moderate or greater. The respective values are 0.209, 0.286, and 0.379. This result is strong evidence indeed, that the degree of irregularity of the temperature lapse rate is directly related to the intensity of CAT.

(5) Maximum lapse rate ( $\gamma_{\max}$ ). The averages computed in °C per 100 ft clearly substantiate the association of CAT with significant inversion layers. The value of 0.259 for moderate CAT is nearly double that computed for the non-turbulence cases.

(6) The maximum vertical vector wind shear ( $\frac{\Delta \vec{V}}{\Delta Z}$ ) shows a relationship to CAT similar to that of the vertical vector wind shear of the central layer. Certainly this variable tends to compensate for those cases where perhaps due to temporal or spatial differences, the reported CAT was just above or below a layer of significant wind shear.

(7) Absolute value of lapse rate in the central layer  $|\gamma|$ . The values (in °C per 100 ft.) of 0.079 for none and 0.062 for very light CAT contrast well with 0.101 obtained for light CAT and 0.134 for moderate CAT. This result definitely points to the conclusion that large positive or negative lapse rates are associated with significant CAT.

#### Comparison With Computations in the Troposphere

A large number of research studies have been conducted over the past 15 years in which the objective has been to relate values of meteorological variables determined from temperature and wind soundings to CAT occurrence in the upper troposphere. In the majority of cases, routine operational radiosonde and rawinsonde data were used. While results frequently indicated a relationship between various parameters indicative of vertical wind shear and stability variations and turbulence, the degree of the relationships or correlations was often modest.

In view of the extent of previous research with synoptic data in the upper troposphere, it was deemed advisable to devote only a minor portion of the effort in the current study to this aspect of the CAT research. A principal objective of this portion of the study was to obtain values of meteorological variables associated with the subjective tropospheric CAT for comparison with the values obtained in association with

CAT in the stratosphere. The formulation of the variables, computational procedures and data format are the same in both sets of computations. It should be remembered that the tropospheric sample is from the January to June 1966 period in the United States while the stratosphere sample encompasses a longer time period and a greater variety of geographic locations. In spite of these differences, it is worthwhile to at least briefly compare the average values obtained in the two sets of computations.

The average values of nine variables associated with CAT in the upper troposphere (generally between 30,000 and 37,000 ft) are given in Table 3-3. The values and the number of cases on which the computations are based are given for intensities of light-to-moderate, moderate or greater and light-to-moderate or greater. These values may be compared with those obtained in association with occurrences and non-occurrences of CAT in the stratosphere given in Table 3-1.

An examination of Table 3-3 shows that there is little systematic variation between the values obtained for light to moderate intensities (19—22 cases) as compared to the values obtained of  $\geq M$  intensities (24 or 25 cases). This is hardly surprising since the sample size is small, the intensities are subjectively determined and the CAT intensity characterizing each case is the most representative (most frequently reported) of 3 to 5 or more subjective reports. All cases of CAT of light to moderate or greater intensity are therefore combined in the table for comparison with computations from stratospheric data.

A comparison of Tables 3-1 and 3-3 shows that the average values associated with light to moderate and greater CAT vary as follows:

(a) The vertical vector wind shear values are very similar in both the upper troposphere and the stratosphere.

(b) The average values of mean wind speed and gradient of kinetic energy are more than twice as large in the upper troposphere. However, note that the average value of maximum wind speed is about  $30 \text{ ft sec}^{-1}$  greater for the tropospheric sample reflecting a higher percentage of winter-middle latitude cases.

(c) The several measures of lapse rate reflect the obvious differences in stability between the troposphere and stratosphere, with the minimum lapse rate in the troposphere being more negative and the maximum lapse rate less positive.

TABLE 3-3

AVERAGE VALUES OF METEOROLOGICAL VARIABLES  
ASSOCIATED WITH CAT IN THE UPPER TROPOSPHERE

Variable	CAT Intensity					
	Light to Moderate		Moderate or Greater		Combined Intensities	
	Average	Cases	Average	Cases	Average	Cases
$\frac{\Delta \vec{V}}{\Delta Z}$	0.825	19	0.642	24	0.723	43
$\bar{V} \cdot \frac{\Delta \vec{V}}{\Delta Z}$	117.4	19	90.2	24	102.3	43
$\bar{V}$	161	19	118	24	138	43
$WS_{\max}$	194	20	141	24	164	44
$\gamma$	-0.213	22	-0.176	25	-0.194	47
$\gamma_{\max} - \gamma_{\min}$	0.333	22	0.398	25	0.367	47
$\gamma_{\min}$	-0.236	22	-0.248	25	-0.243	47
$\gamma_{\max}$	0.096	22	0.113	25	0.105	47
$R'_i$	10	19	15	24	13	43

It is interesting to note though that the average value of the difference between the maximum and minimum lapse rates within  $\pm 6500$  ft of the level of CAT occurrence was very similar for both samples.

In summary, although one can only draw guarded conclusions because of sample size and other sample limitations discussed above, the average values of the vertical vector wind shear and a measure of lapse rate irregularity ( $\gamma_{\max} - \gamma_{\min}$ ) computed for cases of light-to-moderate and more intense CAT were similar in both the troposphere and stratosphere.

#### Relationships of Meteorological Variables to CAT

Another method of determining the relationship between categories of CAT and meteorological variables is to determine the distribution of CAT occurrences for the sample stratified according to prescribed ranges of a variable. The results obtained from a three category classification are shown for ten variables in Table 3-4. The distribution is given for three categories of CAT grouped as none and very light, light, and light to moderate or more intense. The sums of the number of cases will not agree among variables because of missing data. The category limits given in the second column from the left were chosen by considering both the mean category values given in Table 3-2 and the distribution of the individual values tabulated by turbulence category. While the limits are not to be considered optimum it is doubtful that they could be adjusted drastically and still maintain a sufficiently large number of cases in each category. For several variables, more than one set of limits was examined. The variables in the table are listed in order of decreasing percentage of hits in the contingency tables.

All variables show a significantly different distribution of cases in the three CAT categories as one shifts from the lower to upper variable classification. An outstanding example is the vertical gradient of kinetic energy, where for values less than  $25 \text{ ft}^2 \text{ sec}^{-2}$  per 100 ft, 63 of the 89 cases are none or very light and only 11 light to moderate or greater. For values greater than  $40 \text{ ft}^2 \text{ sec}^{-2}$  per 100 ft, only 9 of 43 cases are none or very light and 17 of the cases are light to moderate or greater in intensity. Another striking example is  $\gamma_{\min}$  for which 57 of 87 cases are none or very light and only 7 light to moderate or greater for values greater than  $-0.09^\circ\text{C}$  per



TABLE 3-4  
CONTINGENCY TABLE COMPARISON OF METEOROLOGICAL VARIABLES AND  
CLEAR AIR TURBULENCE

Variable	Category limits	Turbulence cases			Category cases	Total cases	Percent hits	Chi square
		None and very light	Light	Light to moderate or greater				
$\bar{V} \cdot \frac{\Delta \vec{V}}{\Delta Z}$	< 25	63	15	11	89	165	53.9%	33.0
	25-40	19	9	5	33			
	> 40	9	17	17	43			
$(\bar{V} \cdot \frac{\Delta \vec{V}}{\Delta Z})_{\max}$	< 35	61	17	11	89	168	52.4%	18.8
	35-65	21	14	11	46			
	> 65	10	10	13	33			
$\gamma_{\max}$	< 0.15	57	21	17	95	176	47.7%	7.0
	0.15-0.25	17	12	7	36			
	> 0.25	19	11	15	45			
$\gamma_{\min}$	> -0.09	57	23	7	87	175	47.4%	22.8
	-0.09- -0.15	22	8	14	44			
	< -0.15	14	12	18	44			
R'imi	> 25	41	11	4	56	166	45.2%	20.8
	5-25	33	15	11	59			
	< 5	17	15	19	51			
$\gamma$	< 0.060	51	21	15	87	174	44.8%	14.3
	0.060-0.120	25	9	5	39			
	> 0.120	17	13	18	48			
$\gamma_{\max} - \gamma_{\min}$	< 0.25	49	22	13	84	175	44.0%	13.2
	0.25-0.37	27	9	7	43			
	> 0.37	17	12	19	48			
$\frac{\Delta \vec{V}}{\Delta Z}$	< 0.5	51	19	11	81	165	42.4%	17.0
	0.5-0.7	25	4	7	36			
	> 0.7	15	18	15	48			
$(\frac{\Delta \vec{V}}{\Delta Z})_{\max}$	< 0.70	50	18	9	77	165	42.4%	11.5
	0.70-0.95	25	8	12	45			
	> 0.95	16	15	12	43			
$(\frac{\Delta \vec{V}}{\Delta Z})_{\text{lower}}$	< 0.575	29	15	9	53	99	41.4%	3.1
	0.575-0.775	12	4	5	21			
	> 0.775	10	7	8	25			

100 ft. For values less than  $-0.15^{\circ}\text{C}$  per 100 ft., 18 of 44 cases are light to moderate or greater in intensity.

A chi square test was applied to the category distributions of each of the 10 contingency tables. This test is a simple, but certainly only approximate means of evaluating the relative strength of the relationships between the categorized variables and the three categories of CAT. The test essentially measures the departure of the actual category distribution from the number that would be expected based on the row and column totals of the table. Allowing for the proper degrees of freedom (4, for a  $3 \times 3$  table) one can then reject the hypothesis that the actual distribution was due to chance at a given confidence level. At the 5% and 1% confidence level one can state that the distribution is not due to chance if chi square equals or exceeds 9.5 and 13.3 respectively. What must be kept in mind is that each element of the contingency table is considered equally important whereas we are most concerned with ability of a particular variable for a given set of values to isolate cases of significant CAT of at least light to moderate intensity in the stratosphere.

The results in Table 3-4 generally confirm what one might have expected from the previously discussed average values obtained for each CAT category. The two largest values of chi square were obtained for the vertical gradient of kinetic energy  $(\bar{V} \cdot \frac{\Delta \bar{V}}{\Delta Z})$  of the central larger and the minimum lapse rate ( $\gamma_{\min}$ ). The three other variables for which large values of chi square were computed ( $R'_{\text{limi}}$ ),  $(V \cdot \frac{\Delta \bar{V}}{\Delta Z})_{\max}$ ,  $(\frac{\Delta \bar{V}}{\Delta Z})$  are each strongly correlated to the first two variables.

#### Relationship of Combined Variables to CAT

A logical extension of the analysis is to attempt to develop a method of specifying CAT categories by employing two or more variables jointly. Considering both the nature of the data, and the time available it was decided to restrict this portion of the analysis to combinations of two variables only, with the selection being based largely on those variables that individually exhibited the best correlations with CAT intensity.

The analysis procedure was straightforward. For each of five paired variables considered, all cases with indicated intensity were entered on a graph, the location being determined by the joint values of the variables. After examining the distributions and clusterings of like intensities, three areas were delineated and designated as the inner, middle and outer sections of the graph. These areas were intended to

correspond to the following descriptions:

- Inner—little likelihood of CAT and if encountered the intensity is most likely to be light
- Middle—increased frequency of encountering CAT but the intensity is most often light
- Outer—CAT is likely to be experienced and there is a good possibility that it will be of light to moderate or greater intensity

Two examples of the graphs developed are given in Figs. 3-1 and 3-2. The corresponding cases of CAT for each area are given in Table 3-5 for the two figures shown and for three other variable combinations analyzed. The chi square testing of the contingency tables clearly indicated that the combination  $(V \cdot \frac{\Delta \vec{V}}{\Delta Z}) \times \gamma_{\min}$  yielded the most significant distribution. The chi square value obtained was 47.8 compared to 33.0 for  $\vec{V} \cdot \frac{\Delta \vec{V}}{\Delta Z}$  alone.

#### Case Studies

The statistical summaries of meteorological variables, circulation features and satellite-observed cloud features provide the basic data for interpretation and generalization of guidelines to isolate regions in the stratosphere in which CAT is most likely to occur. A more intensive study of particular cases however can provide considerable understanding of the mechanisms producing CAT and help in the concrete formulation of guidelines to predict the phenomenon. Reports of CAT occurrences and non-occurrences for eight dates (April 1, 1966; May 13, 1966; August 24, 1966; August 29, 1966; September 30, 1966; October 20, 1966; October 24, 1966; and October 28, 1966) are discussed. For four of these dates, the discussion is limited to a summary. Further details for these dates and illustrative figures are contained in the second [19] and third [20] quarterly progress reports.

#### April 1, 1966 (Moderate Turbulence)

The HICAT research flight T-54 on April 1, 1966 was conducted from 1825—2225 GMT from Edwards AFB, California. The flight track shown in Fig. 3-3 was through Nevada to extreme southeast Idaho, with the return through Utah, western Wyoming, south to northwest New Mexico, and westward through northern Arizona. The most

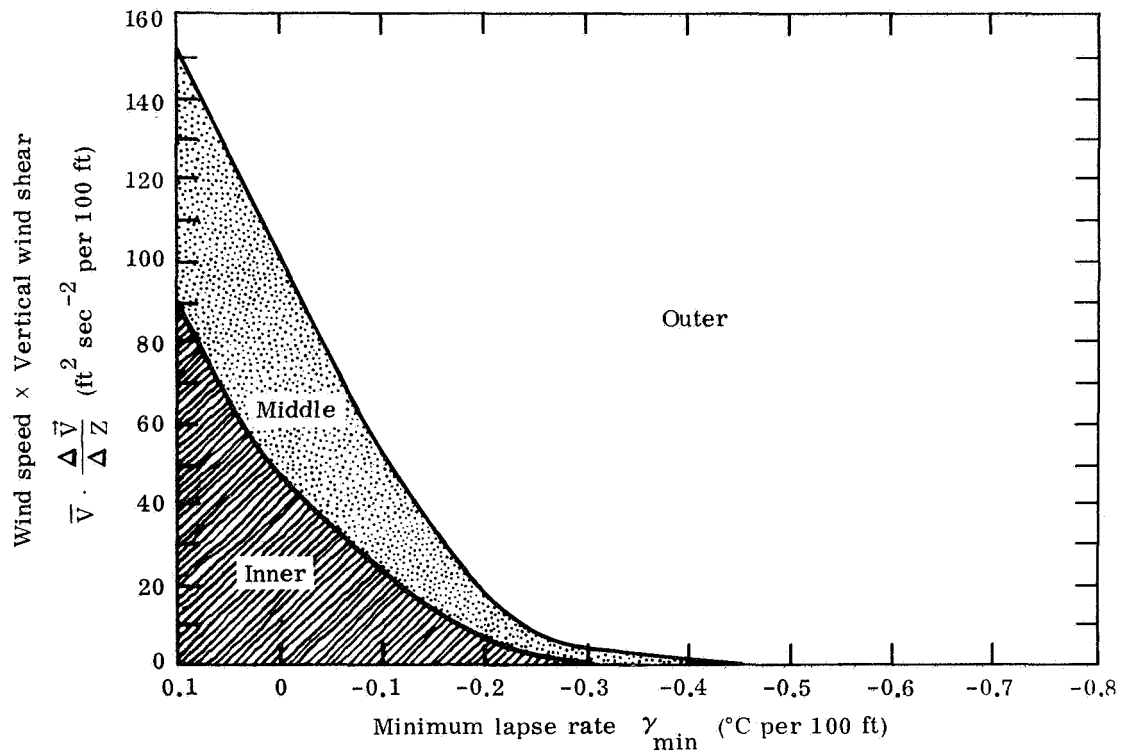


Fig. 3-1. Graph of  $\bar{V} \cdot \frac{\Delta \vec{V}}{\Delta Z} \times \gamma_{\min}$  for determining CAT likelihood.

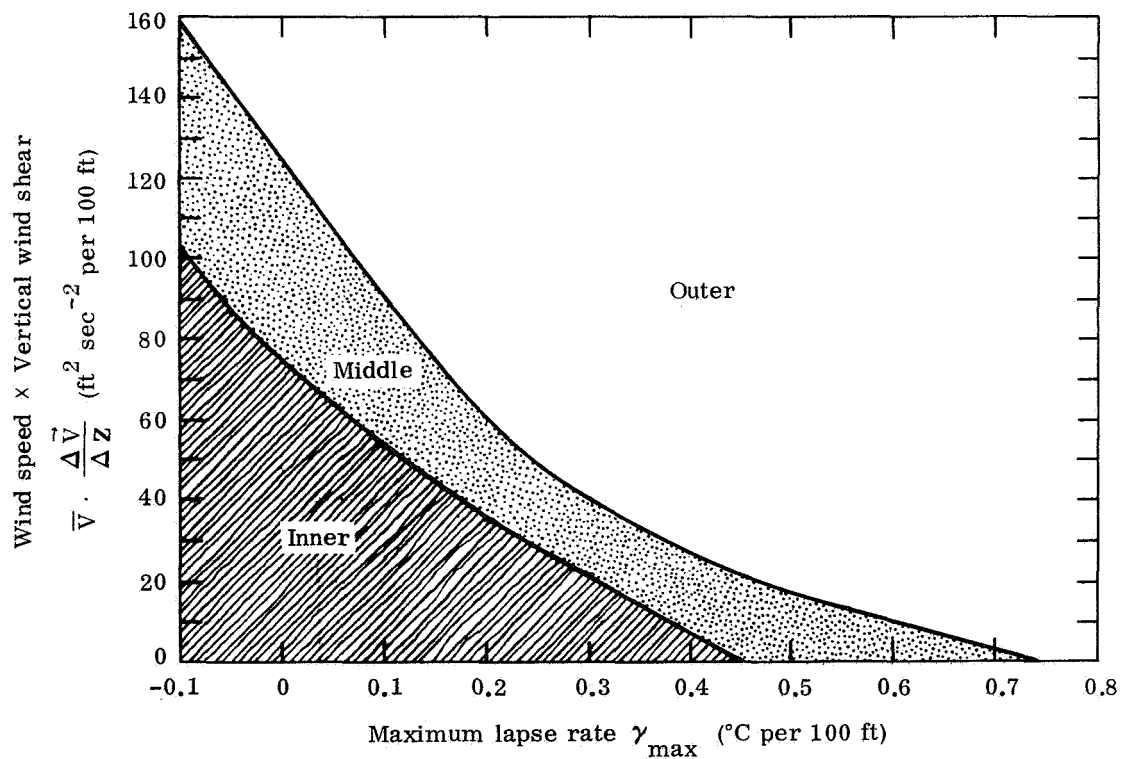


Fig. 3-2. Graph of  $\bar{V} \cdot \frac{\Delta \vec{V}}{\Delta Z} \times \gamma_{\max}$  for determining CAT likelihood.

TABLE 3-5

## CONTINGENCY TABLE COMPARISON OF JOINT VARIABLES AND CLEAR AIR TURBULENCE

Variable	Area category	Turbulence Intensity			Category cases	Total cases	Percent hits	Chi square
		None and very light	Light	Light to moderate or greater				
$\bar{V} \cdot \frac{\Delta \vec{V}}{\Delta Z}$ × $\gamma_{\min}$	inner	64	17	7	88	165	59.4	47.8
	middle	18	12	4	34			
	outer	10	11	22	43			
$\bar{V} \cdot \frac{\Delta \vec{V}}{\Delta Z}$ × $\gamma_{\max}$	inner	72	21	14	107	164	61.0	32.4
	middle	11	15	6	32			
	outer	7	5	13	25			
$(\frac{\Delta \vec{V}}{\Delta Z})_{\max}$ × $\gamma_{\max} - \gamma_{\min}$	inner	61	19	7	87	158	55.7	28.2
	middle	9	7	8	24			
	outer	17	10	20	47			
$\frac{\Delta \vec{V}}{\Delta Z}$ × $\gamma_{\min}$	inner	50	17	6	73	163	50.9	27.3
	middle	22	10	5	37			
	outer	17	13	23	53			
$\bar{V} \cdot \frac{\Delta \vec{V}}{\Delta Z}$ × $\gamma_{\max} - \gamma_{\min}$	inner	42	14	2	58	159	47.2	21.3
	middle	40	19	16	75			
	outer	4	8	14	26			

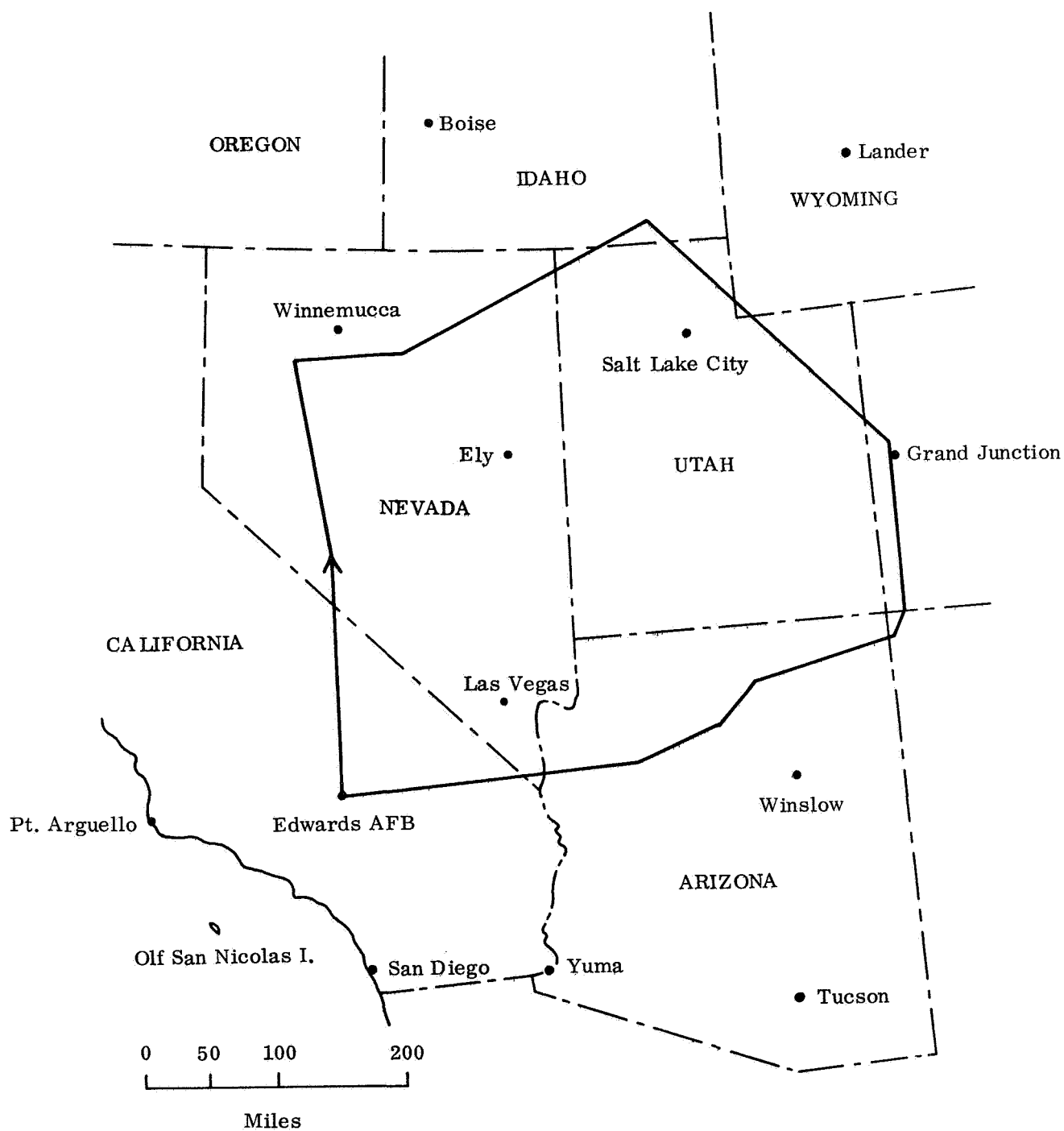


Fig. 3-3. HICAT research flight T-54 on April 1, 1966 from 1825 - 2225 GMT [9].

significant turbulence was reported on the final westward portion of the flight with intensities of light to moderate 75 miles north of Winslow at 54,000- to 55,000-ft altitude and moderate at 60 miles south of Las Vegas at 54,800-ft altitude. There were five subjective reports of light to moderate or moderate CAT at altitudes from 28,000 ft to 41,000 ft between 0400 and 1800 GMT in the region near northern Arizona and southern Utah. Further east in northern Texas and Oklahoma, numerous encounters of CAT of moderate or greater intensity were reported by commercial pilots.

At 0000 GMT of April 2 a southwest-northeast oriented occluded front extended from northern California to western Montana with a weak high-pressure area ahead of the front. A thermal low pressure region extended from Mexico, into eastern California, having associated surface temperatures in the mid-nineties. Surface wind speeds were generally light, reflecting the weak pressure gradients.

At 0000 GMT of April 2, a broad ridge at 300 mb dominated the region of interest, with a closed contour centered about 35°N off the California coast. The ridge extended well into south central Canada. A jet stream plunging down the eastern side of the ridge produced  $160 \text{ ft sec}^{-1}$  wind speeds over the Plains states. In the local area of interest, wind directions were northwest over Nevada and Wyoming and from the north over Arizona.

At 0000 GMT on April 2 a well-developed trough at 100 mb lies over the western quarter of North America with the ridge line centered just west of the Pacific coast. The wind flow is generally from the northwest and is light in the area of interest. Significant horizontal gradients of wind and temperature are found west of the continental divide, but not in the area of the HICAT flight. The 100-mb analysis made by the Free University of Berlin [17] does indicate that the isotherms and height contour fields are somewhat out-of-phase at the 100-mb constant pressure surface.

ESSA 2 photos reveal almost no cloud features of interest in the immediate region of the HICAT flight. There are generally clear conditions with only the gray background evident over the southwestern United States. Cirrostratus is reported over northern Nevada and Utah by ground observers and the HICAT report notes a cirrus overcast present in northern Utah. This is not discernible in the satellite picture which probably indicates the thin, transparent nature of these upper-tropospheric

clouds under northwesterly flow. Further east, banded frontal cloudiness with evidence of cirrus streaking extends to about 95°W near 35°N, a region of many reports of moderate or more severe CAT in the upper troposphere.

Moderate CAT occurred at 2159 GMT in a region 60 miles south of Las Vegas at 54,500 ft. This is precisely the level of the upper tropopause reported in the Las Vegas temperature sounding shown in Fig. 3-4(a). The approximate layer of interest ( $\pm 6000$  ft) is indicated by a hatched box. This region of the atmosphere is characterized by a pronounced temperature inversion and sharp turning of the wind direction with altitude ( $312^\circ$  at 54,100 ft and  $345^\circ$  at 58,500 ft). A strong layer of decreasing temperature with height is noted above the tropopause inversion.

Other portions of the HICAT flight route through Nevada, northern Utah and western Wyoming are characterized only by a few scattered patches of light CAT. The temperature soundings at Grand Junction, Colorado and Salt Lake City, Utah are uniform and near-isothermal in the stratosphere in the vicinity of the layer of reported light CAT.

#### August 24, 1966 (No Turbulence)

HICAT research flight T-113 on August 24 was conducted from Edwards AFB, California during the time period between 1700 GMT and 2241 GMT. The flight was exceptionally wide-ranging, extending to east-central Montana in the northeast and extreme southeastern Washington in the northwest. Other states under or very close to the flight track were California, Nevada, Arizona, Utah, Colorado, Wyoming, Idaho and Oregon. No turbulence was encountered anywhere between the altitudes of 50,000 and 65,000 ft.

At the surface at 1800 GMT on August 24, winds and pressure gradients were extremely weak. An insignificant stationary front extended from Idaho southeastward to extreme northeastern Arizona. In the upper troposphere at the 300-mb surface, contour curvature was anticyclonic over the entire flight path, associated with a well-developed ridge over the western United States. A closed low off the Pacific coast was within  $10^\circ$  longitude of non-occurrence cases on the return leg of the flight over Oregon and Nevada. At the 100-mb constant pressure surface, the contour curvature was again anticyclonic but the most significant feature was the very weak temperature



gradient analyzed over the entire western United States. Cloudiness ranged from clear to scattered to broken patches of cumulus and cirrus with occasional bandedness.

The temperature profiles at all soundings along the flight path were quite smooth. The sounding taken at Boise, Idaho at 0000 GMT of August 25 shown in Fig. 3-4 (b) is a good example. Here, as at several other locations, although the wind speed was fairly strong in the upper troposphere ( $105 \text{ ft sec}^{-1}$  at the 200-mb level), wind speeds decreased rapidly with elevation well below the flight level. Thus, the wind speed decreased only from 23 to  $13 \text{ ft sec}^{-1}$  between 100 mb and 80 mb and the computed vertical vector wind shear was  $0.21 \text{ ft sec}^{-1}$  per 100 ft. There was almost no change in lapse rate within  $\pm 6500 \text{ ft}$  of flight level.

In summary, the cases of no turbulence observed on August 24, 1966 were characterized by

- (1) light wind speeds near flight level,
- (2) weak scalar or vector vertical wind shears,
- (3) weak or non-existent horizontal temperature gradients,
- (4) extremely uniform and stable lapse rates, and
- (5) little cloudiness.

The meteorological conditions in the stratosphere on this date are good examples of those frequently encountered at mid-latitudes during the summer season. The lack of turbulence associated with these conditions is what one would expect and illustrates why CAT encounters would be expected to be at a minimum during the summer.

#### May 13, 1966 (Moderate Turbulence)

HICAT research flight T-75 was conducted from May 13 2101 GMT to May 14 0128 GMT from Hickam AFB, Oahu, Hawaii. No turbulence was encountered on the first leg of the flight to the southwest of the islands over open water. However, approximately 50 miles to the east of Hilo (Hawaii) moderate CAT was encountered at an altitude of 60,000 ft. On the return leg of the flight no turbulence was encountered over or near the islands of Maui, Molokai and Oahu. Thus, the sounding at Lihue, approximately 100 miles to the northwest, was associated with no turbulence.

At the 300-mb constant pressure surface, the circulation features were not significant. The contour curvature was nearly straight, and no pronounced trough, ridge or

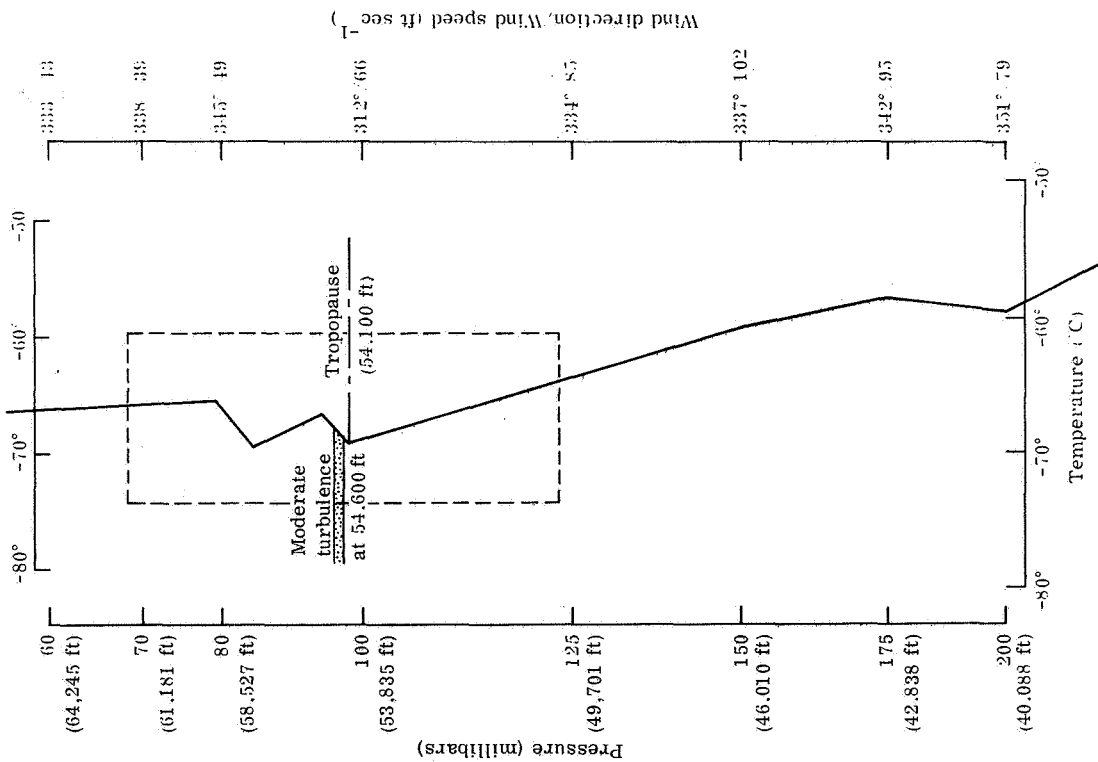


Fig. 3-4(a). Sounding at Las Vegas, Nevada on April 2, 1966 at 0000 GMT. The moderate turbulence was located about 60 miles from the sounding and was encountered 2 hours prior to the observation.

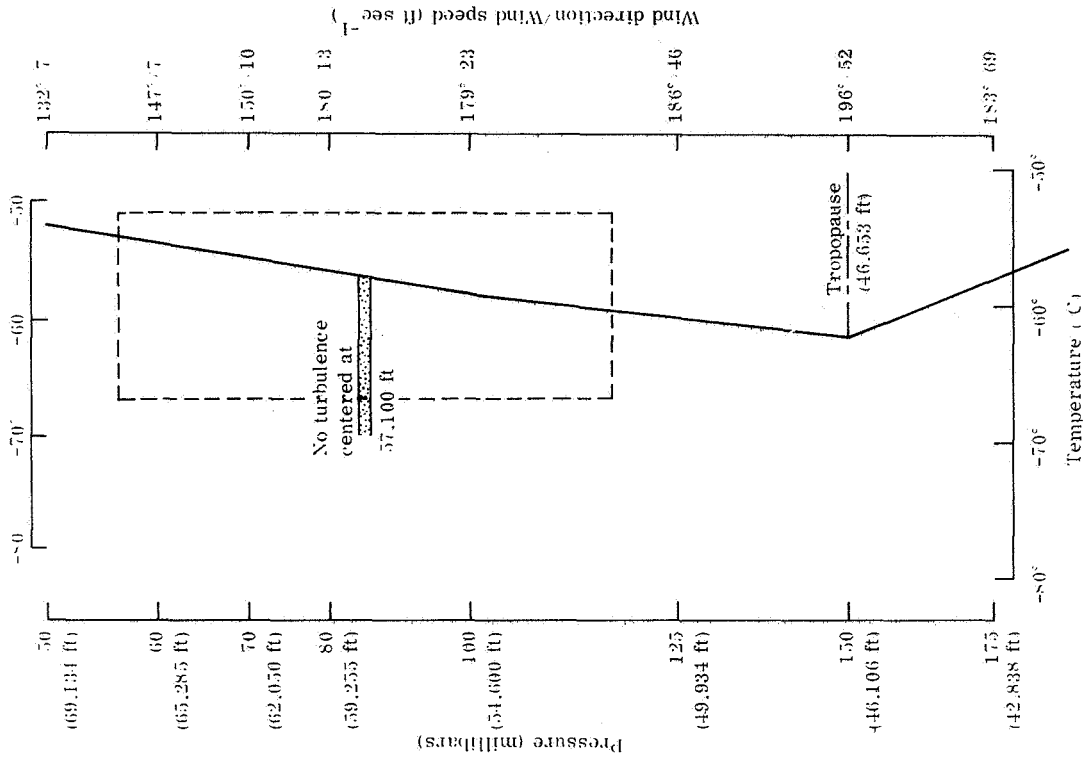


Fig. 3-4(b). Sounding at Boise, Idaho on Aug. 25, 1966 at 0000 GMT. The lack of turbulence was reported 80 miles from the sounding location and 3 hours prior to the observation.

closed low was in the vicinity. However, at 100 mb, both cases (Lihue—no CAT and Hilo—moderate CAT at 59,700 ft) were located in anticyclonic curvature behind a ridge line. The isotherms of the temperature field were analyzed to cross 100-mb height contours, indicating advection was taking place and the temperature gradient at this level was moderate.

The moderate turbulence occurred over a region in which the ESSA 2 photo shows hollow cumuliform cells. The path with no turbulence on the return flight was along the northeast edge of the location of a larger solid connective cell which existed six hours earlier and may or may not have existed at flight time.

The two cases studied on this date help to illustrate a rather important point. The circulation features tabulated for the turbulence and no turbulence cases are practically identical, yet the moderate turbulence was encountered at only a single location. However, significant differences will be seen in the two radiosonde observations taken at Lihue and Hilo. Thus, while circulation features in many instances will give an indication of the possibility of CAT occurring, the individual soundings give a more detailed specification of the likely region of occurrence.

The temperature sounding taken at Hilo on May 14 at 0000 GMT is shown in Fig. 3-5 (a). The temporal and spatial differences between the sounding and the turbulence are quite small. The sounding was taken slightly more than one hour after moderate CAT was observed and only approximately 50 miles distant from the location of the turbulence.

Both the plotted sounding and the numerical computations obtained reveal several significant features. First, the moderate CAT located at 59,700 ft is near the top of a pronounced inversion and just below a layer of significant temperature decrease in an otherwise stable lower stratosphere. The inversion layer centered at 59,140 ft has a positive lapse rate of  $0.30^{\circ}\text{C}$  per 100 ft, while the layer of decreasing temperature with altitude has a negative lapse rate of  $-0.11^{\circ}\text{C}$  per 100 ft. This large variation in lapse rate is particularly significant since the layers are adjacent and embedded in a layer of large vertical vector wind shear. The computed shear was  $1.53 \text{ ft sec}^{-1}$  per 100 ft, much of this being due to the rapid change in wind direction between the 80-mb and 70-mb constant pressure surfaces ( $219^{\circ}$  at 80 mb and  $127^{\circ}$  at 70 mb).

The temperature and wind observations taken at Lihue on May 14, 1966 at 0000 GMT are shown in Fig. 3-5 (b). The temperature sounding and other data show some interesting, if somewhat subtle, differences from the data at Hilo. Again, the time of the sounding and the time of observed no turbulence are almost concurrent. The intervening distance is about 100 miles, still quite reasonable. Notice that a significant inversion of  $0.29^{\circ}\text{C}$  per 100 ft is centered at 55,070 ft, close to the aircraft level at which no CAT was encountered. However, in this sounding there is no layer having a rapid decrease in temperature with height. A negative lapse rate of  $-0.01^{\circ}\text{C}$  per 100 ft centered at 57,300 ft is the layer of least stability within  $\pm 6500$  ft of flight level. Thus, for this sounding the absolute difference between the maximum and minimum lapse rates within  $\pm 6500$  ft of the non-occurrence was  $0.30^{\circ}\text{C}$  per 100 ft and the two layers were widely separated. By contrast the absolute difference for the Hilo sounding was  $0.44^{\circ}\text{C}$  per 100 ft and the layers were adjacent. A final comment to be made is that the vertical vector wind shear was only  $0.59 \text{ ft sec}^{-1}$  per 100 ft with little variation in wind direction between the 100-mb and 80-mb constant pressure surfaces.

In summary, the sounding associated with moderate turbulence [ Fig. 3-5 (a)] possessed the following characteristics not observed in Fig. 3-5 (b):

- (1) a layer with a significant decrease in temperature with height,
- (2) a sharply irregular lapse rate with a strong inversion layer adjacent to the layer with a negative lapse rate, and
- (3) a large vertical vector wind shear including significant change in wind direction with altitude.

#### September 30, 1966 (Moderate Turbulence)

HICAT research flight T-126 from Hanscom Field, Massachusetts was conducted over northern New England and New York State from 1354 GMT to 1728 GMT on September 30, 1966. Although there was some uncertainty regarding the exact location of the flight track, moderate turbulence was determined from the instrument and subjective pilot report to have occurred over southern Maine and northern New York State. The moderate CAT over Maine was encountered about 1430 GMT in the altitude range 49,200 to 58,100 ft and was associated with the sounding taken at Portland Maine, about 20 miles distant. The moderate CAT over New York State was observed at about

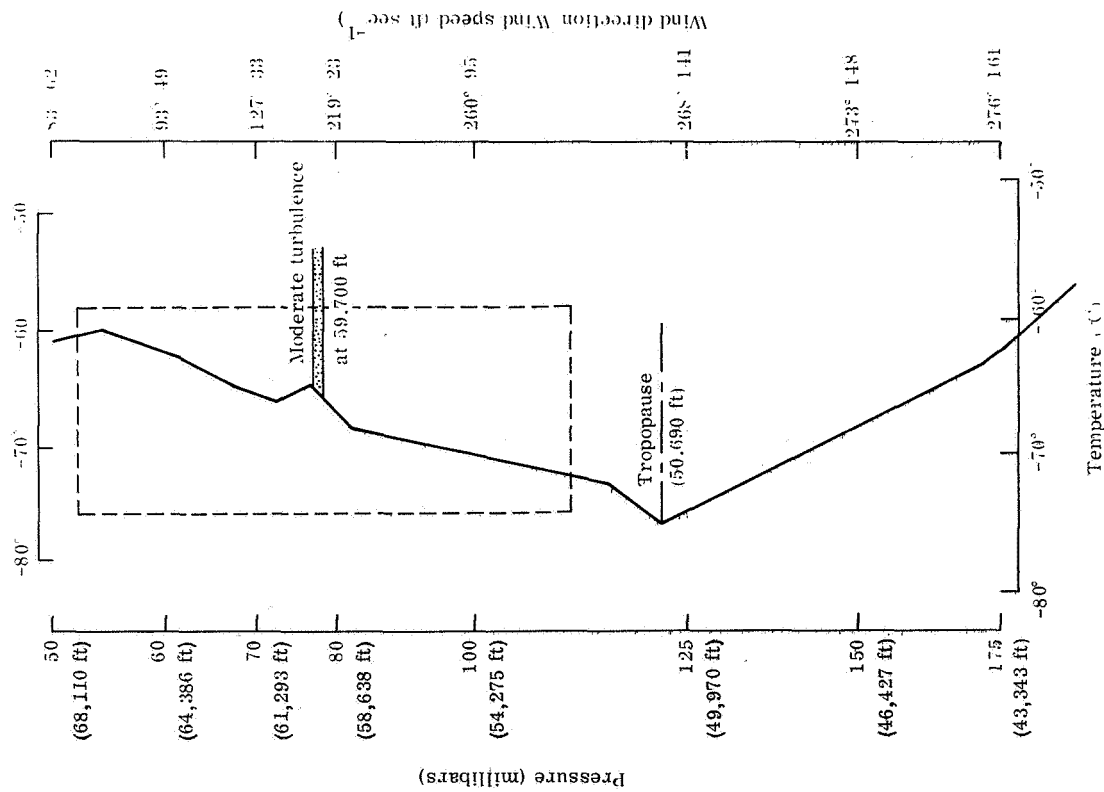


Fig. 3-5(a). Sounding at Hilo, Hawaii on May 14, 1966 at 0000 GMT. The moderate turbulence was located about 50 miles from the sounding and was encountered 1 hour prior to the observation.

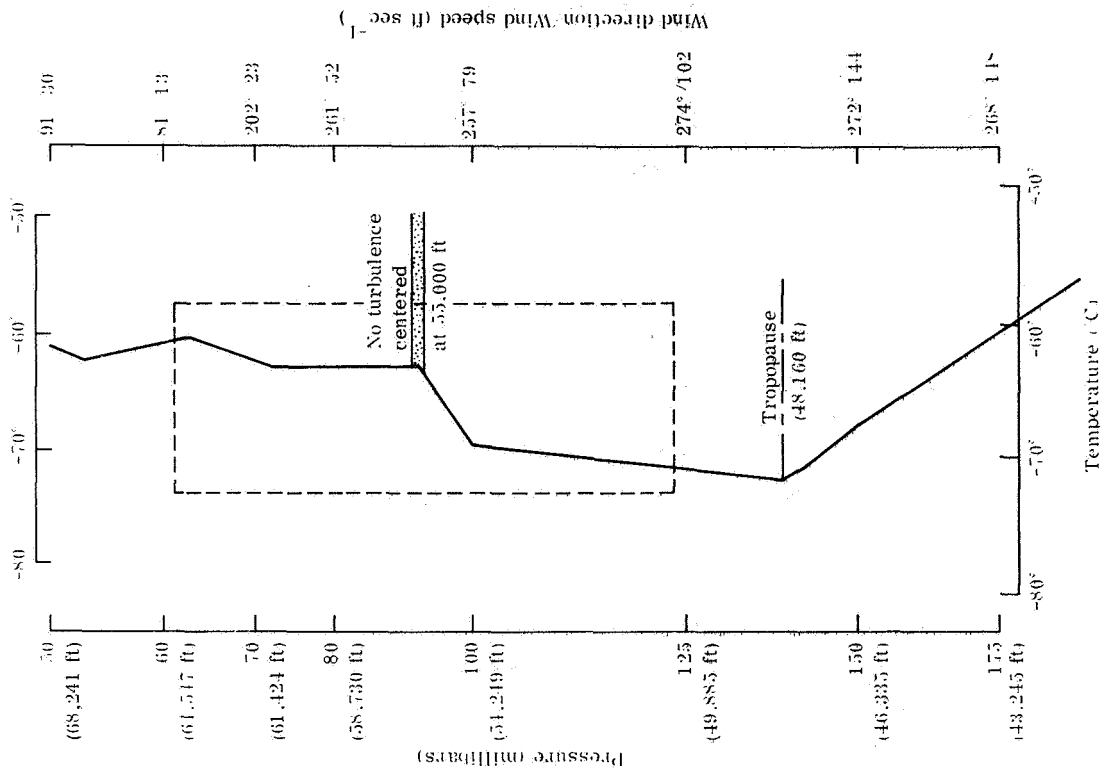


Fig. 3-5(b). Sounding at LiHue, Hawaii on May 14, 1966 at 0000 GMT. The lack of turbulence was reported 100 miles from the sounding and one-half hour prior to the observation.

1530 GMT in the altitude band between 49,200 and 52,500 ft and was matched with the sounding taken at Albany resulting in a separation of about 80 miles between the CAT and sounding location.

At the surface on September 30 at 1200 GMT a vigorous 984 mb low was centered just north of New York State with strong cyclonic, westerly flow at the surface over New England. The associated cold front was well off the coast. The cyclone was almost vertical in structure, as a closed low at 300 mb was present in southeastern Canada within  $10^\circ$  longitude of both moderate CAT occurrences. The contour curvature at 300 mb was cyclonic in the region of interest. At the 100-mb constant pressure surface the contour curvature was essentially straight, with little cyclonic tendency, and the isotherm field was parallel to the contour flow with a moderate temperature gradient. The cyclonic vortex was the most striking photographic feature, with the turbulence over Maine at the south edge of the solid vorticular mass. The turbulence over upper New York, was near cumuliform and cirrus bands, the former spiralling into the vortex.

Both temperature soundings taken at 1200 GMT of September 30 at Portland shown in Fig. 3-6 (a) and at Albany shown in Fig. 3-6 (b) are quite irregular in shape in the altitude region about the layers of moderate CAT. At Portland, there is a double temperature inversion structure with an intervening layer of strongly negative lapse rate. The upper inversion layer, the base of which is defined as the tropopause, is within the turbulent layers while the lower inversion layer is just below the region of moderate turbulence. The upper temperature inversion centered at 50,320 ft has a lapse rate of  $0.37^\circ\text{C}$  per 100 ft and the difference in maximum and minimum lapse rates within  $\pm 6500$  ft of the center of the layer of moderate CAT is a very large  $0.56^\circ\text{C}$  per 100 ft. The vector vertical wind shear between 125 mb and 100 mb is a substantial  $0.79 \text{ ft sec}^{-1}$  per 100 ft. The vector shear of the layer below this central layer is larger, being  $0.95 \text{ ft sec}^{-1}$  per 100 ft.

At Albany a single temperature inversion of  $0.28^\circ\text{C}$  per 100 ft centered at 52,470 ft is within and slightly above the turbulent layer. Again, strong negative lapse rates are found directly above and somewhat below the inversion layer. The difference between maximum and minimum lapse rates is  $0.45^\circ\text{C}$  per 100 ft. Unfortunately,

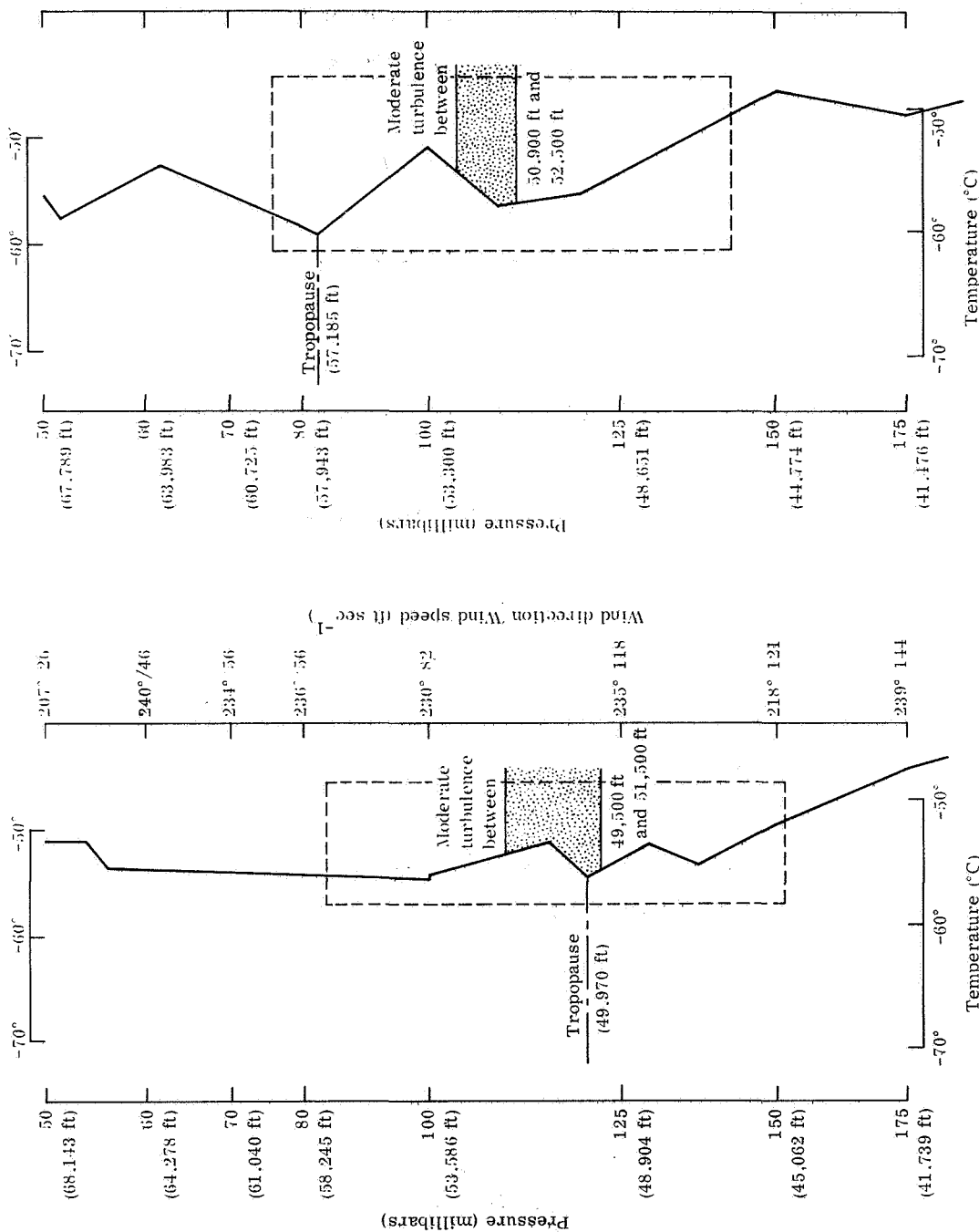


Fig. 3-6(a). Sounding at Portland, Maine on September 30, 1966 at 1200 GMT. The moderate turbulence was located about 20 miles from the sounding and was encountered 2 hours after the time of observation.

Fig. 3-6(b). Sounding at Albany, N. Y. on September 30, 1966 at 1200 GMT. The moderate turbulence was located about 80 miles from the sounding and was encountered three and one-half hours after the time of observation.

as is too often the case when significant CAT is encountered, the wind data are missing. The highest level reporting is 400 mb with a speed of  $187 \text{ ft sec}^{-1}$ , indicating a very strong flow.

The latter two cases again strongly emphasize the association between irregular temperature lapse rates (alternating positive and negative lapse rates in the vertical about the CAT layer) and significant CAT.

Case studies of other HICAT flights are summarized below. These cases are on August 29, 1966; October 20, 1966; October 24, 1966; and October 28, 1966. On all days except October 20 (light to moderate CAT) at least moderate turbulence was encountered.

The August flight was out of Edwards AFB, California, and primarily over and near the lee of the Sierra Nevada. The flight path including four instrumented encounters with moderate CAT, was partly over a surface front, cold to stationary with a satellite picture showing banded cumulus and altocumulus. Winds at 500 mb ahead of a coastal trough reached  $82 \text{ ft sec}^{-1}$  from the southwest over Nevada. Near 175 mb the wind was southwest at  $138 \text{ ft sec}^{-1}$ . Winds were also southwesterly and parallel to the isotherms at 100 mb. Soundings nearby showed at least slightly irregular temperature profiles near 100 mb.

The October flights were all from Hanscom AFB, Massachusetts, and over or near the jet stream. Turbulence ranged from light to moderate on October 20 to moderate on the other days. Upper tropospheric and stratospheric flow were southwesterly on October 20 and 24, and westerly on the 28th. On October 20 the ESSA 2 picture showed transverse wave clouds near the light to moderate CAT occurrence. On October 24 the moderate CAT occurred near a region of banded altocumulus and cirrus. On October 28 one occurrence of moderate CAT was just  $1^\circ$  south of a distinct frontal band while another was over an area of clear skies.

#### Summary of CAT Relationships with Meteorological Variables

To briefly summarize, the results of the analysis of the relationships between CAT in the stratosphere and meteorological variables have shown the following:

Large differences between the maximum and minimum lapse rates within  $\pm 6500\text{-ft}$  of the level of interest are indicative of an irregular rate and significant CAT.



Large negative values of the minimum observed lapse rate (layer of rapidly decreasing temperature) and large positive values of the maximum observed rate (a strong inversion) are both related to significant CAT. Besides being indicative of an irregular lapse rate, a strong temperature inversion is associated with locally large vertical wind shear, while a layer of rapidly decreasing temperature with height is a region of decreased stability in a normally near-isothermal or stable stratosphere.

Although wind data are reported in less detail than is desirable, large values of the vertical vector wind shear centered on the level of interest are clearly associated with a more frequent incidence of significant CAT. Large vertical wind shear and especially a large vertical gradient of kinetic energy is associated with rapid transfer of momentum or "overtuning" of the atmosphere. The resulting eddy fluctuations or perturbations are experienced by aircraft as CAT.

The joint consideration of the vertical gradient of kinetic energy  $(\bar{V} \cdot \frac{\Delta \vec{V}}{\Delta Z})$  in conjunction with the minimum observed lapse rate ( $\gamma_{\min}$ ) most clearly isolates the probable occurrence of light to moderate or more intense CAT in the stratosphere for the sample analyzed.

## B. Satellite Television and Infrared Data

The cloud features appearing in weather satellite television pictures which may be of importance relative to stratospheric turbulence are described below. Figure 3-7 is a conceptual model of significant cloud features, outlined in rather idealized fashion relative to the jet stream and to a surface frontal system. Many authors, particularly Whitney, et al. [21], Crooks, et al. [9], and Viezee, et al. [11] have contributed to the summarized information.

### Characteristics of Satellite Video Data

Vortical clouds—Cyclonically-curved bands of predominantly middle (8,000—18,000 ft above the surface) and low (less than 8,000 ft above surface) spiralling in toward a region close to the center of a low-pressure system.

Banded frontal clouds—elongated (may be 500—1000 miles or more) bands of bright, thick-appearing clouds associated with cold or occluded fronts, usually having a horizontal thickness of several hundred miles.

Cirrus bands—elongated bands of cirrus clouds (30,000—45,000 ft above the surface) are often found on the southern side (to the right, looking down stream) of the jet stream.

Sharp-edged cirrus—The northern edge of the cirrus, when well-defined, is often close to the jet stream core, or location of maximum wind speed. Above (and below) this region, large vertical wind shears are found and often associated with CAT.

Shadow line cast by the cirrus on lower middle cloudiness, when the sun angle is favorable, also defines the edge of a cirrus band.

Cirrus streaks or narrow bands—while less reliably associated with jet stream activity, do reveal the direction of the upper tropospheric or lower stratospheric wind field. The general appearance may give indications of circulation characteristics.

A break in a cirrus band locates a region of organized and extensive downward vertical motions and likely vertical overturning and turbulent exchange.

Transverse wave clouds are frequently nearly perpendicular to the direction of the flow. The alternative cloudy and clear regions correspond to the upward and downward motions in a wave, which is often terrain-induced. This cloud, at cirrus levels,

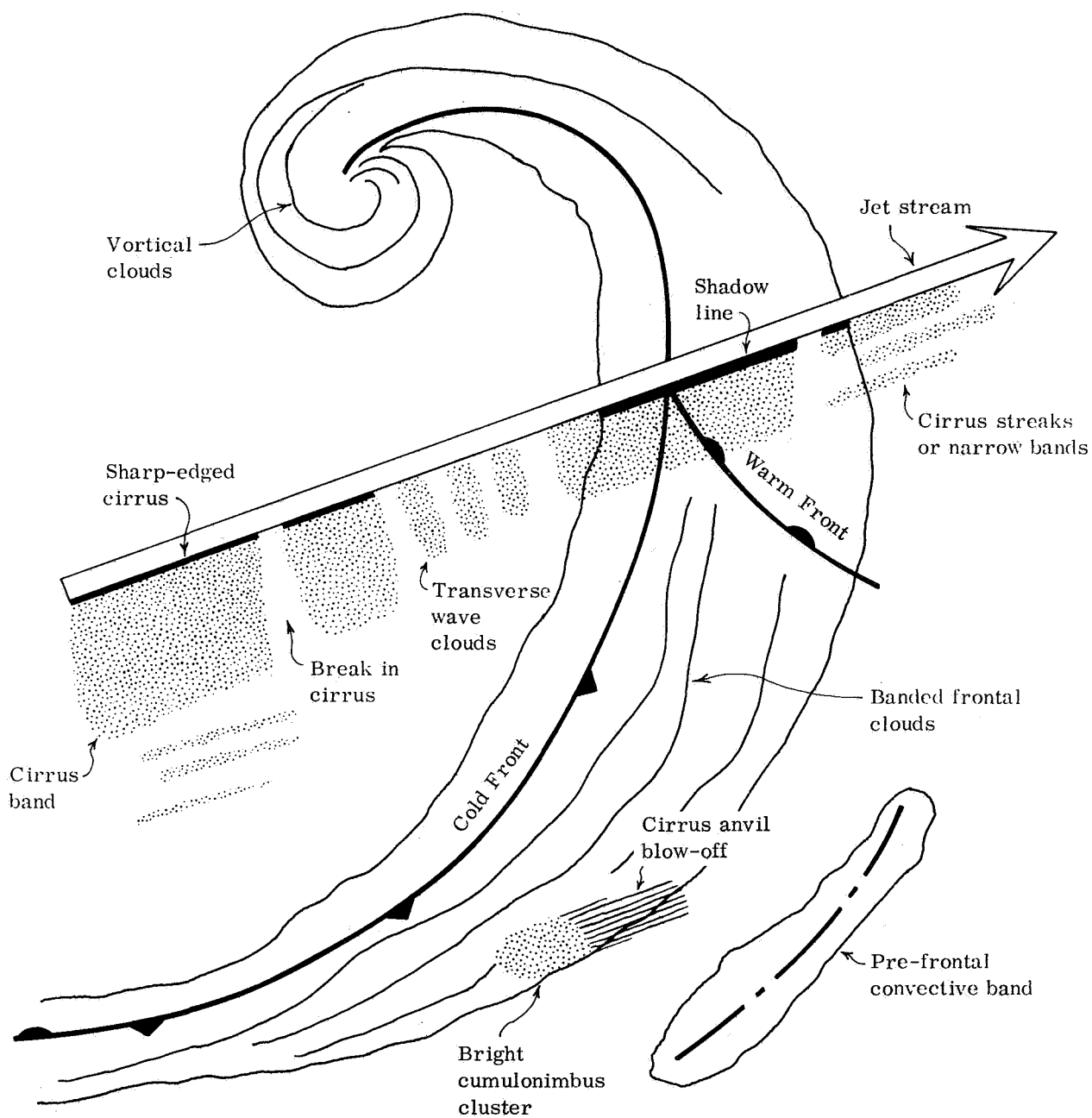


Fig. 3-7. Idealized characteristics of satellite video data.

indicates a potentiality of upward propagations of disturbances well into the stratosphere.

Bright cumulonimbus cluster is composed of several cumulonimbus clouds, the tops of which in cases of strong convective activity, may extend well into the stratosphere to 50,000 ft or higher. The cirrus anvil blowoff associated with mature clouds provides information on wind direction and an estimate of wind speed. Turbulence may be found in clear air, well removed from the thunderstorm cloud. Cumulonimbus clouds, as well as being associated with frontal systems, occur in unstable air masses and in pre-frontal convective bands ahead of the frontal system.

Fronts (boundaries between air masses), convective clouds, and the jet-stream-tropopause region can be considered barriers in somewhat the same sense as terrain and may be associated with the generation of upward-propagated wave activity. These features, then, may be associated with turbulence at higher levels as well as in their immediate vicinity. Hence, cloudiness associated with these features is of interest for locating them in conventional data-sparse regions and revealing circulation characteristics, particularly on a small scale.

Other cloud patterns are observed in the course of the study, but it will be shown later that these conditions are more likely to be related to little or no stratospheric turbulence. These are:

Broken to overcast (usually irregular) patches of mostly stratiform cloudiness;

Cumuliform cells (hollow or solid), when apparently capped by a mid-tropospheric inversion; and

Areas of clear skies or scattered clouds (not banded).

Distance of the turbulent region from the visible cloud feature is also important with regard to the strength of the turbulence. Cloud features were examined within five degrees latitude or longitude of the CAT observation point for selection of the major cloud feature. For this reason the most severe CAT occurrence on a given day was first selected, then other CAT cases only if they were more than 5° longitude distance from each other. An example of a satellite photograph used in the study is given in Fig. 3-8.

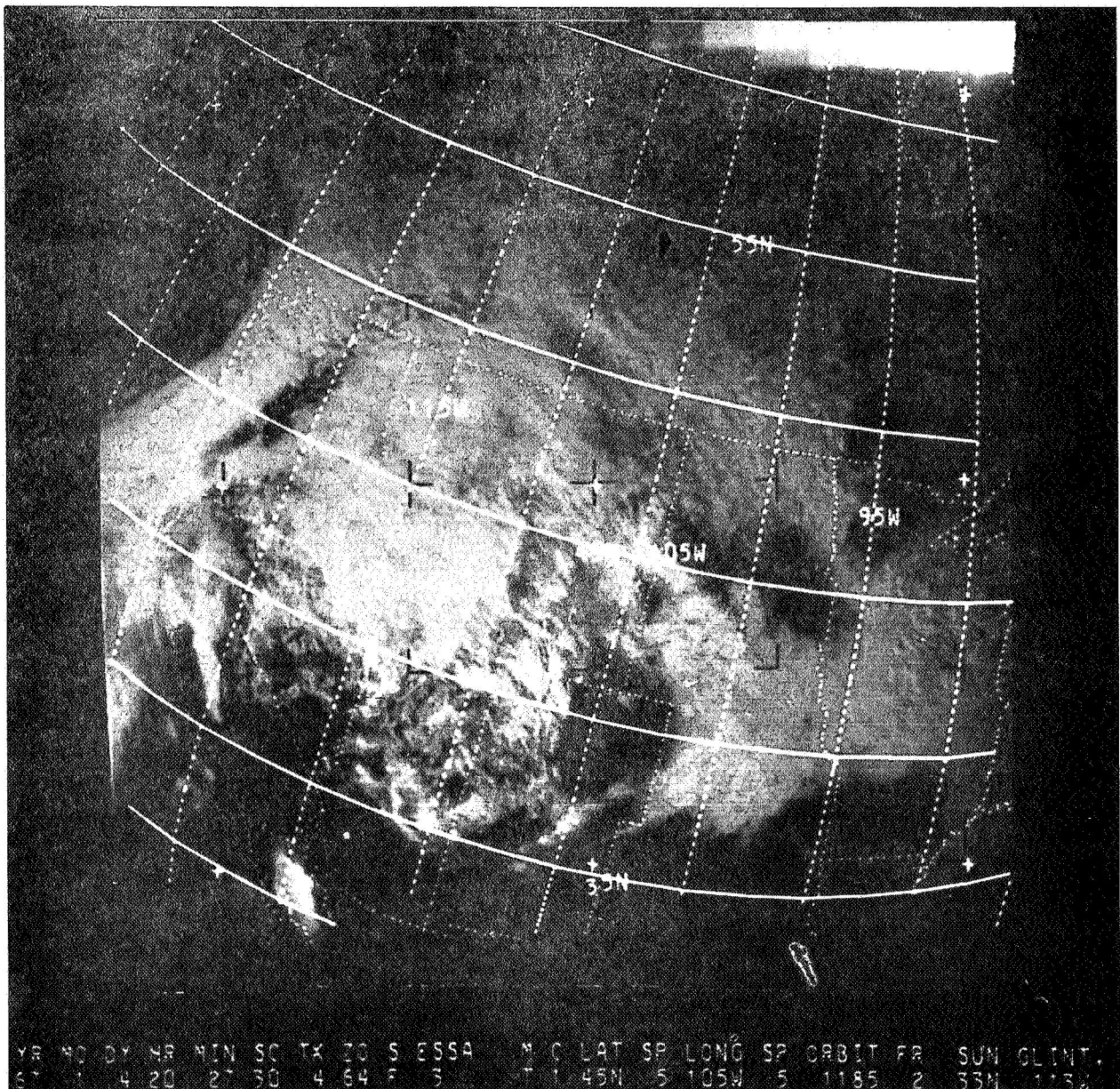


Fig. 3-8. ESSA 3 picture on Jan 4, 1967 (2028 GMT) showing small wave clouds at 39°N, 116° to 118°W, nearly transverse to the 400 mb wind of 267°, 102 ft sec<sup>-1</sup> measured at Ely, Nevada (0000 GMT, Jan 5, 1967) about 150 miles to the east. The pilot on the HICAT flight gave a subjective report of moderate CAT at 39°N, 118°W at an altitude of 54,000 ft.

The comparison of major cloud fields from satellite video pictures with two exhaustive categories of Phase 2 HICAT observations is given in Table 3-6. For the most part categories 1 to 8 of major cloud features are related to none to light turbulence. Categories 9 to 14 are related in this sample to a greater percentage of occurrence of light to moderate or greater turbulence.

TABLE 3-6  
MAJOR TELEVISION FEATURES OF HICAT OBSERVATIONS  
FREQUENCY SUMMARIZED BY CLOUD CATEGORY

Major cloud features	Number of CAT cases	
	None through light	Light to moderate or greater
1. None to scattered clouds	22	1
2. Broken to overcast St, Sc, Ac/As, Cs	8	0
3. Convective Cu-form and Ci > 2° away	6	0
4. Edge of Cb and Ci	4	0
5. Over frontal cloud mass or band	3	0
6. Edge of broad frontal cloud mass	7	0
7. Edge of frontal cloud band	1	3
8. Edge of vortex	7	2
9. Broken patches of Cu, Ac, Ci with Cs	3	2
10. Straight or curved Ac, Ci, Cu-form bands ≤ 2° away	6	5
11. Convective Cu-form cells, Ci bands ≤ 2° away	2	2
12. Wave clouds	0	1
13. Over major vortex	1	1
14. Over Cb	1	2
Totals	71	19

Cloud abbreviations used in Tables 3-6 and 3-7 are:

St - Stratus	Cs - Cirrostratus
Sc - Stratocumulus	Cu - Cumulus
Ac - Altocumulus	Ci - Cirrus
As - Altostratus	Cb - Cumulonimbus

A chi square value of 28.34 was obtained from the  $14 \times 2$  table. The probability that the categories are unrelated is only one per cent.

With respect to the individual lines of the table, the five per cent probability level for chi square with one degree of freedom is 3.841. The only calculated chi squares which exceed this are for cloud categories 1, 7 and 10. Thus, "None to scattered clouds" is significantly related in this sample to occurrence of none to light turbulence in the stratosphere. The "edge of a frontal cloud band" is significantly related to light to moderate or greater turbulence. The occurrence of at least light to moderate stratospheric turbulence within  $2^\circ$  latitude or longitude of bands of cumulus or altocumulus with cirrus bands also appeared to be significant. The apparent significance is assumed from the chi square test indicating unlikely random occurrences of the frequencies in these three categories. For other individual cloud categories, there were too few cases to define relationships.

On only nine days comprising 26 cases were there Nimbus II HRIR temperature values available at the HICAT data locations. Analyzed 35 mi square average effective radiating temperature values in this  $3.5\text{--}4.1\mu$  band at these locations ranged from 246°K to 298°K. If the cooler radiators were solid overcast cloud masses, these temperatures would represent cloud tops ranging from over 20,000 ft to near sea level. The warmest temperatures, in fact, represent radiation from the earth's surface with clear skies. In only about one-third of these cases using average HRIR values was there a likely match between the IR value and the cloud condition observed about ten hours later. Values of radiation received by the HRIR device over an area of scattered to broken cloudiness represent an integration of radiance from the earth's surface and various cloud tops, attenuated slightly by the intervening atmosphere. The effective temperature determined from the satellite data thus has to be warmer than the temperature of the coldest cloud top. In this small sample there is no apparent relationship

between the HRIR temperature values and the occurrence of turbulence. However, in six cases these temperature values do confirm that the cloudiness apparent in the pictures extends above 10,000 ft.

The sample of upper tropospheric commercial and military reports of turbulence from ESSA was also compared with the satellite photos in the manner described above. As noted earlier this sample consisted only of reports of light to moderate or greater turbulence. In the Phase 2 HICAT sample (Table 3-6) 68% of the light to moderate or greater cases occurred with cloud categories designated 9 through 14. Only 33% of the ESSA CAT cases fell within cloud categories 9, 10, 12 and 13 as shown in Table 3-7.

TABLE 3-7  
OBSERVATIONS (FROM ESSA) OVER OR NEAR  
MAJOR SATELLITE TELEVISION CLOUD FEATURES<sup>1</sup>

Number <sup>2</sup>		Number of CAT cases		
		Light to moderate	Moderate	Moderate to severe
1	None to scattered clouds	1	1	0
2	Broken to overcast St, Sc, Ac/As, Cs	3	2	0
3	Convective Cu-form and Ci > 2° away	0	1	1
4	Edge of Cb and Ci	1	0	0
5	Over frontal cloud mass or band	0	4	1
6	Edge of broad frontal cloud mass	1	1	0
7	Edge of frontal cloud band	2	1	0
8	Edge of vortex	1	0	0
9	Broken patches of Cu, Ac, Ci with Cs	2	2	0
10	Straight or curved Ac, Ci, Cu-form bands ≤ 2° away	1	1	0
12	Transverse wave clouds	0	3	1
13	Over major vortex	1	1	0
15	Cs edge, probable jet stream	1	2	0
Totals		14	19	3

<sup>1</sup>Ten cases (Feb. 1966) from cloud analysis.

<sup>2</sup>Numbered to correspond with HICAT cloud classes.



Cloud categories 11 and 14 did not occur at all with the ESSA sample. On the other hand, in the ESSA sample three reports occurred near an apparent jet stream cloud formation. This category did not occur with the Phase 2 HICAT sample.

In summary, clear skies, scattered clouds, or irregular nearly overcast masses of generally stratiform clouds are usually associated with no turbulence to light turbulence in the stratosphere. On the other hand, it appears that the probability of light to moderate or greater CAT becomes significant near banded cumulus, altocumulus and cirrus, over cumulonimbus, and near transverse wave clouds in the lee of rough terrain. If the significant cloud feature is more than 140 mi away, little or no turbulence is usually expected.

### C. Atmospheric Circulation Features

A tabulation of circulation features (Table 3-8) was performed for all cases involving occurrence and non-occurrence of CAT in the stratosphere as defined from the HICAT sample—Phase 2. The tabulation was not performed for the cases defined from the subjective reports in the upper troposphere. This region has been the subject of research for many years. The tabulation was intended to be as brief and simple as possible, since all cases in the stratosphere were to be examined. The objective was to determine the extent of synoptic associations existing between CAT and smooth air in the stratosphere and principal circulation features at the surface, 300 mb, and 100 mb. The analyses used in most cases were those published by the Free University of Berlin [16, 17] which are every 24 hours. For some cases six-hourly surface charts from the National Meteorological Center were available. An attempt was made to allow for temporal changes in circulation features. Since the difference in time between the turbulence occurrence or non-occurrence and the meteorological analysis may be up to 12 hours and was on the average about 6 hours, a sophisticated scheme for associating the CAT with circulation features was clearly not warranted.

The tabulation categories are defined below:

#### Surface Analysis

(a) Presence of frontal boundary at the surface within 5° longitude of location of occurrence or non-occurrence: Yes or No.

(b) Presence of cyclone center within 10° longitude of location: Yes or No.

#### 300 mb Analysis

(a) Contour Curvature—Cyclonic; Anticyclonic; or Straight

(b) Position relative to trough and ridge lines:

- within ~5° longitude of trough line; ahead of trough
- within ~5° longitude of ridge line; behind ridge
- within ~5° longitude of ridge line; ahead of ridge
- within ~5° longitude of trough line; behind trough
- none of the above

(c) Within 10° longitude of closed low (closed contour): Yes—No.

TABLE 3-8  
PERCENT FREQUENCY DISTRIBUTIONS OF CIRCULATION FEATURES STRATIFIED  
ACCORDING TO CAT INTENSITY

CAT Intensity	Surface				300 mb												
	Front		Cyclone		Curvature				Trough-Ridge						Closed low		Total cases
	Yes	No	Yes	No	Cyclonic	Anti-cyclonic	Straight	Behind trough	Ahead of trough	Behind ridge	Ahead of ridge	None	Yes	No			
None and very light	73	27	40	60	55	32	13	13	13	34	12	16	26	24	76	95	
Light	68	32	45	55	43	27	30	2	27	7	11	52	16	84	44		
≥ Light to moderate	78	23	55	45	55	28	18	13	28	20	5	35	30	70	40		
Overall distribution	72	28	45	55	52	30	18	10	31	12	12	35	24	76	179		

CAT Intensity	100 mb															Total cases
	Curvature				Trough-Ridge					Isotherm			Temperature gradient			
	Cyclonic	Anti-cyclonic	Straight	Behind trough	Ahead of trough	Behind ridge	Ahead of ridge	None	Cross-contour	Wave shape	Parallel to contour	Weak	Moderate	Strong		
None and very light	50	27	23	15	26	9	13	37	34	24	42	52	41	7	95	
Light	40	31	29	16	26	10	7	41	36	28	36	24	71	5	44	
≥ Light to moderate	44	31	25	6	22	11	6	55	45	20	35	25	53	22	40	
Overall distribution	46	29	25	13	25	10	10	42	37	24	39	39	51	10	179	

### 100 mb Analysis

Note that the 100 mb surface is normally located near 53,000 ft while the 50 mb surface is usually located at about 68,000 ft. Thus, for most flights, the 100 mb surface is closer to the level of occurrence and is, in general, to be considered the level of greater interest for all occurrences under 62,000 ft. The 70-mb constant pressure surface analyses were not available.

- (a) Contour Curvature—Cyclonic; Anticyclonic; Straight
- (b) Position relative to trough and ridge lines:
  - within  $\sim 5^\circ$  longitude of trough line; ahead of trough
  - within  $\sim 5^\circ$  longitude of ridge line; behind ridge
  - within  $\sim 5^\circ$  longitude of ridge line; ahead of ridge
  - within  $\sim 5^\circ$  longitude of trough line; behind trough
- (c) Characteristic of Isotherm Field (smoothed)
  - Generally parallel to height contours
  - Wave-like or generally cross ( $\geq 30^\circ$ ) contour flow (advection)
- (d) Temperature gradient (smoothed)
  - $< 4^\circ \text{C}/5^\circ$  longitude (weak)
  - $4$  to  $8^\circ \text{C}/5^\circ$  longitude (moderate)
  - $\geq 8^\circ \text{C}/5^\circ$  longitude (strong)

A certain degree of subjectivity was present in the tabulation of circulation features. This is acceptable considering the smoothed nature of the Berlin analyses, the temporal differences between meteorological and turbulence data and the results obtained provide only "broad" guidance.

Tabulations of the above circulation features were performed for the following categories of CAT intensity:

- (a) none; very light; light; light to moderate; or greater than or equal to moderate
- (b) none to light; light to moderate or more intense.
- (c) none to very light; light; light to moderate or more intense
- (d) none to very light; light or more intense

Initially, the tabulation according to (a) above was performed separately for instrumented and subjective reports. All but three subjective reports of CAT occurrence or non-occurrence have light or less intensity. After an initial examination, a decision was made to consider all cases for larger sample size and greater stability of correlation, as little difference was apparent. The category limits (c) and (d) were compiled for all cases and separately for those cases located above and below 56,000 ft altitude.

The relationships between circulation features and categories of CAT intensity demonstrated by the analysis were modest at best. This is not too surprising considering the broad, general nature of the circulation categories and the moderate sample size. While, as was demonstrated in Section 3(A), the sample size is adequate to develop well-defined relationships between CAT intensity and selected meteorological variables, the generalized nature of the circulation features probably requires a more substantial sample.

In view of the above discussion only tabulation (c) for all cases is shown in Table 3-8. The distribution in terms of percentage is shown for three categories: none to very light; light; and light to moderate or more intense. The total number of cases is given for each category and the overall frequencies are given at the bottom of both sections of the table. It should be noted that for six cases, circulation data for 100 mb was not available and that the number of cases for the three categories of the 100-mb isotherm field exceeds the total on the right-hand side of the table since more than one category can be selected for a given case.

Considering all cases, the variations that seem most consistent are:

A surface cyclone is present 55% of the time when light to moderate or more intense CAT is occurring and only 40% of the time when no turbulence or very light CAT is encountered.

Light to moderate or more intense CAT rarely occurred behind the 100-mb trough (6% of cases) or ahead of the 100-mb ridge (6% of cases). Since these essentially represent the same region of the circulation, the statistics reinforce each other.

The 100-mb isotherm field is more frequently out of phase with the contour flow when light to moderate or more intense CAT is occurring.

Probably of greatest significance, strong 100-mb temperature gradients occur 22% of the time when light to moderate or more intense CAT is encountered and only 7% of the time when no turbulence or very light CAT is present. The temperature gradient was classified as weak 52% of the time with no turbulence. In comparison (table not shown) of cases above and below 56,000 ft altitude, it was noted that CAT of light to moderate or greater intensity is encountered more frequently below (26 of 93 cases) than above (14 of 86 cases) the 56,000 ft level. This is in agreement with the results of Crooks, et al. [14] that turbulence in the 60,000 to 70,000 ft altitude band was less severe than in the 50,000 to 60,000 ft band.

A chi square test was made of the contingency table distribution from which each of the percentage frequency groups listed in Table 3-8(a) and (b) were derived. The computed chi squares indicated that at the 5% confidence level, of the 9 circulation features, only the table relating the three categories of 100-mb temperature gradient to CAT intensities contained a distribution that could not be due to chance.

We may summarize the relationship between CAT and circulation features as follows:

Light to moderate or more intense CAT is associated with an increased frequency of large horizontal temperature gradients at 100 mb constant pressure surface and with the isotherm field being out of phase with the contour pattern indicating advection and changing stability. This result is in agreement with the findings of Ashburn, et al. [22].

Concentrations of kinetic energy in the atmosphere as reflected in surface cyclones were found to occur more frequently under regions of turbulence in the stratosphere than when stratospheric flow is smooth.

Light to moderate CAT in the stratosphere was not clearly related to the contour curvature or the trough-ridge positions at the 300-mb surface. Significant CAT is infrequent in the region ahead of the 100-mb ridgeline and behind the trough. The result with respect to the 300-mb surface is not in agreement with Crooks, et al. [4] who state that "HICAT

tests indicate that turbulence is abundant above regions of pronounced cyclonic curvature of a strong jet stream and moves near the speed of the axis of the jet stream trough." This contradiction may be more apparent than real since our analysis did not differentiate between degrees of strength of cyclonic curvature and the results obtained by Crooks, et al. reflect Phase 3 HICAT tests as well as those conducted during Phase 2. The Phase 3 tests include a large number of flights from Edwards AFB, California from November 1967 through February 1968 in which CAT was encountered. Our analysis sample did not include as extensive a number of flights in mid-latitude in the winter season (flights in New Zealand and Australia were excluded). This points to the desirability of the currently continuing program to include the HICAT Phase 3 data.





#### 4. LOCATING PROBABLE REGIONS OF CLEAR AIR TURBULENCE

Modern turbulence theory views the problem in terms of a continual cascade of energy from long wavelength flow (general circulation) to very small-scale transient circulations of the microscale. All intermediate scales are important since the energy dissipation is viewed as continuous (spectral analysis) without any "gap." An aircraft, depending on its size, design and cruising speed, will of course be sensitive only to a particular wavelength interval. To predict the likelihood of an aircraft encountering turbulence, however, one must be aware of atmospheric conditions over a broader scale of motion. To generalize the problem, one is concerned with locating regions of the atmosphere where significant potential or kinetic energy is present and there exists a mechanism (thermal instability or shearing of the flow) to convert or dissipate this energy toward a smaller scale in an abrupt manner and at a non-uniform rate resulting in fluctuations of the flow and CAT. With these background remarks in mind, let us consider the prediction procedure primarily from the following viewpoint: the satellite data and circulation features provide information on the general level of energy while the sounding data indicates the presence of a conversion mechanism.

In formulating a procedure for locating or predicting CAT in the stratosphere we must be cognizant of several considerations. The results of research performed in this study and elsewhere provide both general insights and specific relationships between CAT occurrence and environmental characteristics. The procedures developed are dependent on data availability and quality, and operational constraints in using the data. There are a variety of user requirements and for example we were particularly aware of the need to provide a basis for the development of specific design criteria for detection instrumentation.

A set of guidelines for locating regions of CAT should start with a realization of the climatological information available regarding CAT occurrence. The most relevant and recent climatological studies of CAT in the stratosphere have been compiled from analyses of HICAT data by Ashburn, et al. [22] and Crooks, et al. [14]. From their analysis, Ashburn, et al. determined the percentage of flight miles in turbulence over mountains (height of terrain greater than 3000 ft) to be 6.9%, while over flat lands (height less than 3000 ft) and over water the percentage was 5.5%. If only

moderate or more intense CAT is included the percentages are for mountains 2.1%, for flatlands 1.8% and for water 1.0%. Crooks, et al. [14] in a somewhat different analysis compared for all HICAT tests, the percentage of turbulence runs with the percentage of flight time in terrain categories of water, flat lands (relief difference less than 2500 ft) and mountains (relief difference greater than 2500 ft). The results are:

	<u>Water</u>	<u>Flat lands</u>	<u>Mountains</u>
Percentage of flight time	27%	37%	36%
Percentage of turbulence runs	11%	41%	48%

Not only is CAT more frequently encountered over land than water but the likelihood of the turbulence being of moderate or severe intensity is greater.

Crooks, et al. [14] also analyzed the frequency of CAT occurring in 5,000 ft bands from 45,000 to 70,000 ft. The data pointed to "a possible increase in the occurrence of turbulence in the 50,000 to 55,000 ft band when all bases are considered" and decreasing frequency above that layer.

What the above indicates is that prior to examining current data one is a priori somewhat more concerned with airspace over mountainous terrain under 55,000 ft than with airspace over oceans above 55,000 ft. The examination of current data can, however, considerably alter these climatological expectancies.

The general procedure for locating regions of CAT in the stratosphere is as follows:

(1) From an examination of features contained in circulation analyses and satellite pictures one determines those regions where the occurrence of CAT is most likely (centers of kinetic energy) and also indicate regions where CAT occurrence is least probable. The circulation analysis at the pressure level closest to flight level or layer of interest is, of course, to be particularly studied.

(2) Available radiosonde data is then examined in a sequence dictated by the analysis in (1) both for the general profile of temperature and winds and to obtain quantitative measures of meteorological variables related to CAT occurrence. A

specific objective, of course, is to focus on regions of smaller horizontal and vertical dimension where significant CAT is expected, than is possible from an analysis of circulation or satellite features. In regions where few or no radiosonde observations are available an analysis could be supplemented with temperature data obtained from Satellite Infrared Spectrometer (SIRS) data from the Nimbus 3 satellite, which was designed primarily for obtaining stratospheric and upper tropospheric temperatures.

Circulation Features to be particularly examined are:

Indicators of increased likelihood of CAT occurrence

- Presence of surface cyclone and to a lesser extent frontal boundaries
- Large horizontal temperature gradient at 100-mb constant pressure surface (or constant pressure surface in stratosphere closest to layer of concern)
- Isotherm field out-of-phase with contour pattern at 100-mb surface indicating advection and changing stability.

Indicators of decreased likelihood of CAT occurrence

- Region approximately 5° longitude ahead of ridgeline or behind trough line on the 100-mb constant pressure surface.
- Weak or non-existent horizontal temperature gradients at the 100-mb surface.

Satellite Features to be noted are:

Indicators of increased likelihood of CAT occurrence

- At the edge of or over a frontal cloud band
- Within 140 mi of cumuluform, altocumulus and/or cirrus bands
- Near transverse wave clouds
- Over cumulonimbus

Indicators of decreased likelihood of CAT occurrence

- Area of nearly clear skies (no banded clouds)
- Area of broken to overcast stratiform clouds (no visible bands)
- No cumuliform clouds indicating moderate to strong convection or cirrus bands within 140 miles.

The radiosonde data yielding vertical temperature and wind profiles can be studied subjectively and can be employed to compute numerical measures of meteorological variables using the computer program developed in this study. The variables may be computed relative to a level or series of levels.

The analysis of the sounding data clearly shows that significant CAT in the stratosphere was associated with atmospheric conditions that tend toward greater thermal or kinetic instability and hence the presence of a mechanism to convert larger scale motions to smaller scale turbulent fluctuations. Specifically, light to moderate or more intense CAT is considerably more frequent when

- the temperature lapse about the level of interest is irregular and includes both strong inversions (locally large vertical wind shear) and layers in which the temperature rapidly decreases with the height (a region of decreased thermal stability within a thermally stable stratosphere), and
- the vertical vector shear of the horizontal wind or the vertical gradient of kinetic energy is large with the result that rapid transfer of momentum or "overturning" can occur with the resulting eddy fluctuations or flow perturbations being experienced as CAT.

These conditions were best reflected by numerical results associated with the six variables given below. Also given with each variable are the category limits generally differentiating between the following categories: no turbulence and very light CAT; light CAT; and light to moderate or more intense CAT.

Group 1:

<u>Variable</u>	<u>Limits</u>	<u>Units</u>
$\bar{V} \cdot \frac{\Delta \vec{V}}{\Delta Z}$	< 25 > 40	ft <sup>2</sup> sec <sup>-2</sup> (100 ft) <sup>-1</sup>
$\frac{\Delta \vec{V}}{\Delta Z}$	< 0.5 > 0.7	ft sec <sup>-1</sup> (100 ft) <sup>-1</sup>
$(\bar{V} \cdot \frac{\Delta \vec{V}}{\Delta Z})_{\max}$	< 35 > 65	ft <sup>2</sup> sec <sup>-2</sup> (100 ft) <sup>-1</sup>

Group 2:

<u>Variable</u>	<u>Limits</u>	<u>Units</u>
$\gamma_{\min}$	$< -0.09$ $> -0.15$	$^{\circ}\text{C (100 ft)}^{-1}$
$\gamma_{\max} - \gamma_{\min}$	$< 0.25$ $> 0.37$	$^{\circ}\text{C (100 ft)}^{-1}$
$R'_{\text{imi}}$	$> 25$ $< 5$	—

With each variable, the first limit defines the category associated with no turbulence or very light CAT and the second limit defines the category where light to moderate or more intense CAT is most likely. Notice that Group 1 comprises the wind variables while Group 2 comprises the temperature or temperature and wind variables. It is recommended that one use at least one variable from each group in assessing the likelihood of CAT. The above six variables stress the most significant results obtained from the analysis of CAT occurrence with respect to radiosonde data. Briefly, they are designed to illustrate the following circumstances in which significant CAT in the stratosphere might occur:

- (1) moderate or strong wind speeds and at least moderate values of the vertical vector wind shear,
- (2) large values of the vertical vector wind shear that may occur even in relatively light flow when the wind direction is changing rapidly with height,
- (3) the product of the wind speed and vertical shear (effective gradient of kinetic energy) is large in a layer adjacent to the CAT layer,
- (4) the minimum lapse rate in the layer ( $\pm 6000$  ft) about the level of interest is significantly negative (lower stability) in a generally isothermal or relatively stable stratosphere,
- (5) the difference between the maximum and minimum lapse rates in the layer about the level of interest is large indicating an irregular lapse rate and rapidly changing stability in the vertical, and

(6) the Richardson Number computed with the minimum lapse rate is small demonstrating the presence of both a layer of negative lapse rate and significant vertical wind shear.

A final step in the procedure of seeking to delineate limited regions of probable significant CAT in the stratosphere should involve use of the two graphs given (Figs. 3-2 and 3-3). On these graphs, with axes of  $\bar{V} \cdot \frac{\Delta \vec{V}}{\Delta Z} \times \gamma_{\min}$  and  $\bar{V} \cdot \frac{\Delta \vec{V}}{\Delta Z} \times \gamma_{\max}$  respectively, inner, middle and outer areas are defined. Only when the values of the variable combinations produce an intersection in the outer region was light to moderate or more intense CAT frequently encountered in the Phase 2 HICAT data sample.

## 5. SUMMARY

The guidelines and relationships discussed in this report are not to be construed as final, but reflect our assessment of results. The problem of detecting atmospheric turbulence involves consideration of all scales of motion from large to small micro-scale eddies. All intermediate scales are important since the energy dissipation is viewed as continuous. An estimate of the probability that an aircraft will encounter turbulence, depends on atmospheric conditions over a broader scale of motion than that to which a particular aircraft responds. Clear air turbulence is most likely in unstable regions where the available energy is large. Procedures described in this report for locating regions of CAT consider the energy source and dissipation based on the satellite data and circulation features providing information on the general level of energy and balloon sounding data indicating the presence of a convection mechanism.

From meteorological variables computed from radiosonde observations [Section 3(A)], the important indicators of significant turbulence are:

- (1) product of the mean wind speed and the vertical vector wind shear determined over about a one-mile thick layer
- (2) vertical vector shear alone
- (3) maximum temperature lapse rate
- (4) minimum temperature lapse rate
- (5) difference between (3) and (4)
- (6) an adjusted Richardson number based on the minimum lapse rate.

Light to moderate or more intense CAT is considerably more frequent when the temperature lapse rate about the level of interest is irregular and includes adjacent layers with large positive and negative lapse rates. Layers with large positive lapse rates (inversions) are associated with large vertical wind shear and layers of marked negative lapse rates are regions of decreased thermal stability within a thermally stable or isothermal stratosphere. Furthermore, when the vertical vector shear of the horizontal wind or the vertical gradient of kinetic energy is large, rapid transfers of momentum or "overturning" can occur with the resulting eddy fluctuations or flow perturbations being experienced as CAT.

Cloud features [Section 3(B)] most frequently related to light to moderate or more severe CAT are:

- (1) banded cumuliform or cirrus within 2° latitude distance of the location in question
- (2) transverse wave clouds within 5° latitude
- (3) major vortex cloud mass at the location
- (4) cumulonimbus at the location, or a band of cumulonimbus within 2° latitude
- (5) edge of a cirrostratus sheet indicative of a jet stream within 2° latitude (often forming a shadow line on lower clouds).

From a current constant pressure map [Section 3(C)] , near the flight level, say 100 mb (about 53,000 ft), one would look for (1) a large horizontal temperature gradient, or (2) an isotherm field out-of-phase with the contour pattern, as an indicator of likely turbulence. Stratospheric CAT is more probable over a surface cyclone than over most other identifiable regions of a surface weather map.

Circulation features, satellite cloud pictures, and radiosonde data have been related to instrumented and subjective reports of turbulence. Current analysis of Phase 3 data from U.S. Air Force Project HICAT will further delineate those atmospheric parameters most associated with clear air turbulence for subsequent design of detection instrumentation for aircraft operations.



## 6. REFERENCES

1. National Committee for Clear Air Turbulence, 1966: Report to the federal coordinator for meteorological services and supporting research. U.S. Government Printing Office, Washington, D. C.
2. Boeing Scientific Laboratories, 1968: Symposium on clear air turbulence and its detection. Summary of papers, The Boeing Company, Seattle, Washington.
3. Clodman, J., G. M. Morgan, Jr., and J. T. Ball, 1961: High level turbulence. AWS Technical Report 158 (reprint), Air Weather Service (MATS) USAF.
4. Reiter, E. R. and A. Nania, 1964: Jet-stream structure and clear-air turbulence (CAT), J. Appl. Meteorol., 3, 3, pp. 247—260.
5. Hildreth, W. W., A. Court, and G. Abrahms, 1965: High altitude rough air model study. Technical Report AFFDL-TR-65-112, Lockheed-California Co., Contract No. AF33(657)-11409, Air Force Flight Dynamics Laboratory, Wright-Patterson, AFB, Ohio.
6. Ball, J. T., 1962: A multiple-discriminant analysis of clear-air turbulence. Technical Memo. 7044-42, The Travelers Research Center, Inc., Hartford, Conn.
7. Endlich, R. M., and G. S. McLean, 1965: Empirical relationships between gust intensity in clear-air turbulence and certain meteorological quantities, J. Appl. Meteorol., 4:2, pp. 222—227.
8. United Aircraft Corporate Systems Center, 1967: Research on advanced supersonic aircraft avionics in four specific areas. Contract NAS 12-518, NASA-ERC, United Aircraft Corp., Farmington, Conn.
9. Crooks, W. M., F. M. Hoblit, D. T. Prophet, et al., 1967: Project HICAT, an investigation of high altitude clear air turbulence. Technical Report AFFDL-TR-67-123, 3 Vols., Lockheed-California Co., Contract AF33(657)-11134, A.F. Flight Dynamics Lab., A.F. Systems Command, Wright-Patterson AFB, Ohio.
10. Clodman, J., and J. T. Ball, 1959: Clear air turbulence. Final Report, Research Division, College of Engineering, New York University, Contract No. AF19(604)-3068.
11. Viezee, W., R. M. Endlich, and S. M. Serebreny, 1967: Satellite-viewed jet-stream clouds in relation to the observed wind field, J. Appl. Meteorol., 6:5, pp. 929—935.

12. Dutton, J. A., 1967: Belling the CAT in the sky, Bull. Am. Meteorol. Soc., 48:11, pp. 813-820.
13. U.S. Air Force Systems Command, Flight Dynamics Laboratory, 1967: Critical atmospheric turbulence (ALLCAT).
14. Crooks, W. M., F. M. Hoblit, and F. A. Mitchell, et al., 1968: Project HICAT High Altitude Clear Air Turbulence measurements and meteorological correlations. Tech. Rpt. AFFDL-TR-68-127. Two vols., Lockheed-California Co., and A.F. Flight Dynamics Lab., A.F. Systems Command, WPAFB, Ohio.
15. National Weather Satellite Center, 1965: A. P. T. (Automatic Picture Transmission) Users Guide. Environmental Science Services Administration, Washington, D. C.
16. ARACON Geophysics Co., 1966: Nimbus II Users Guide. Prepared for NASA/GSFC under Contract NAS 5-10114, p. 229.
17. Institut Für Meteorologie und Geophysik der Freien Universität Berlin, 1966: Tägliche Höhenkarten der 100-mb-Fläche sowie monatliche Mittelkarten für das Jahr 1966. Band LXV, Heft 1-4 (4 Vols.), Verlag von Dietrich Reimer in Berlin.
18. Institut Für Meteorologie und Geophysik der Freien Universität Berlin, 1966: Tägliche und mittlere boden- und 300-mb karten der Nordhemisphäre im Jahre 1966. Band LXIV, Heft 1-12, Verlag von Dietrich Reimer in Berlin.
19. Cooley, D. S. and J. T. Ball, 1969: Research to determine cloud and synoptic parameters associated with clear air turbulence. Second Quarterly Progress Report, NASA/ERC Contract NAS 12-699, The Travelers Research Corporation, Hartford, Conn. Conn.
20. Cooley, D. S. and J. T. Ball, 1969: Research to determine cloud and synoptic parameters associated with clear air turbulence. Third Quarterly Progress Report, NASA/ERC Contract NAS12-699, The Travelers Research Corporation, Hartford, Conn.
21. Whitney, L. F., Jr., A. Timchalk and T. I. Gray, Jr., 1966: On locating jet streams from TIROS photographs, Mo. Weath. Rev., 94:3, pp. 127-138.
22. Ashburn, E. V., D. T. Prophet and D. E. Waco, 1968: High altitude clear air turbulence models for aircraft design and operation. Tech. Rpt. AFFDL-TR-68-79, Air Force Flight Dynamics Laboratory, AFSC, WPAFB, Ohio.
23. Anderson, A. D., 1956: Free atmospheric turbulence. U.S. Naval Research Laboratory, NRL Report 4735, Washington, D. C.

## APPENDIX A. SPECIFICATIONS FOR THE COMPUTATION OF METEOROLOGICAL VARIABLES FROM RADIOSONDE AND RAWINSONDE DATA

### 1. Introduction

This specification describes a computer program for an IBM 360/40 computer to compute certain meteorological variables, the values of which are to be associated with occurrences and non-occurrences of clear air turbulence (CAT) in the stratosphere or upper troposphere. The input consists of pressure (P), temperature (T), height (Z), wind direction (WD) and wind speed (WS) data at constant pressure surfaces from 400 mb to 50 mb, for a series of vertical soundings or radiosonde observations (RAOB). The input data is on punched cards and the specified output is printed. It should be noted that all computations in the program are performed in metric units, while the values in the report are given in english units.

### 2. Input

The input data for each sounding has the following order and information:

<u>Card</u>	<u>Description</u>
0	Number of levels of radiosonde data.
1	This card gives the radiosonde station call letter, number, location, and the date and time of observation. Additionally, the associated CAT information will be specified including altitude range, date-time, terrain type, intensity and distance from radiosonde station.
2 to n	The number of cards of this type depends on the number of levels reported in the sounding. Three levels can be included on one card with the variables P, Z, T, WD, WS listed, in that order, at each level. Thus, if 10 levels and one tropopause level (20 columns) are reported, 5 cards of this type are required. 15 levels and two tropopause levels (41 columns) necessitates 6 cards, etc. Card n+1 is always the last card containing tropopause data only.

The detailed format of the above three card types is described below:

<u>Column</u>	<u>Format</u>	<u>Description of card type 0</u>
1—3	^LL	number of levels of radiosonde data
<u>Column</u>	<u>Format</u>	<u>Description of card type 1</u>
1—5	^AAA^	Radiosonde station call letter
6—11	^BBXXX	Radiosonde block number and station number
12—16	^XX.X	latitude (°N) of radiosonde station location
17—21	XXX.X	longitude (°W) of radiosonde station location
22—25	DDMM	day, month (alpha-numeric) of RAOB
26—31	^^YYYY	year (1966 or 1967, currently) or RAOB
32—36	^tttt	time (GMT); either 0000 or 1200 of RAOB
37—42	^h <sub>1</sub> h <sub>1</sub> h <sub>1</sub> 00	lower altitude of CAT layer in meters
43—48	^h <sub>2</sub> h <sub>2</sub> h <sub>2</sub> 00	upper altitude of CAT layer (if 2 levels specified)
49—54	DDHH00	day, hour (00 to 23 GMT) or CAT
55—56	^T	terrain type 1= ocean 2= flat land 3= hills 4= mountains
57—58	II	CAT Intensity 1=none 2=VL 3=L 4=L to M 5=M 6=M to S 7=S (instrument); 11=0 12=VL 13=L 14=L to M 15=M 16=M to S 17=S (subjective)
59—65	^DIS	Approximate distance of CAT from radiosonde station in kilometers.
66—70	^XX.0	Approximate latitude of CAT occurrence (°N)
71—75	XXX.0	Approximate longitude of CAT occurrence (°W)
76—78	^^X	Altitude of turbulence is 1=determined by instrument 2=subjective report of pilot and 3=center level of layer.

All information on this card will be printed out.

## Sounding Data Card

<u>Column</u>	<u>Format</u>	<u>Description of card type 2 to n</u>
1—5	^^PPP	Pressure in mb (400—50) first level
6—11	_hhhhh	Altitude (meters)
12—16	-TT.T	Temperature (°C)
17—21	^^ddd	Wind direction (degrees)
22—26	^^ff	Wind speed (meters per second)
27—31	^^PPP	Pressure in mb (400—50) second level
32—37	_hhhhh	Altitude (meters)
.	.	.
.	.	.
.	.	.
74—78	^^ff	Wind speed (meters per second) third level

Missing data will be left blank in all appropriate columns. For example, missing wind direction is 000, while missing wind speed is 00.

In addition, on a final card n+1 of the sounding, the tropopause(s) pressure(s), height(s) and temperature(s) are listed (20 columns are required for each tropopause level reported).

The format of the tropopause card n+1 is: TRØP $\wedge$  $\wedge$ P<sub>t</sub>P<sub>t</sub>P<sub>t</sub> $\wedge$ h<sub>t</sub>h<sub>t</sub>h<sub>t</sub>h<sub>t</sub>h<sub>t</sub>-TT.T.  
After a blank column, this format is repeated if a second level is present.

### 3. Computations

The computations can be divided into three sections: (a) determine height of those pressure surfaces for which this variable is missing, (b) computations from temperature data and (c) computations from wind data and computations using both wind and temperature data.

### Computation of Missing Height Values

For each sounding:

- Assume 400 mb height is correct.
- Consider all reported levels between 400 mb and 50 mb inclusive.

If height values are missing at any level including significant levels, these will be determined as follows:

(1) Note the first pressure level above 400 mb at which the height value is missing.

(2) Take the average of the temperature at this level (i + 1) and the temperature at the next lower level (i) at which the height is available:

$$T_j = \frac{1}{2} (T_{i+1} + T_i)$$

where subscripts i and i + 1 designate adjacent reported pressure levels, and subscript j designates the layer between them. Convert  $\bar{T}$  to °K:  $\bar{T}(^{\circ}\text{K}) = \bar{T}(^{\circ}\text{C}) + 273.16$

(3) Compute the thickness,  $\Delta Z_j = 28.818 \bar{T} \ln \frac{P_i}{P_{i+1}}$

(4) Then  $Z_{i+1} = Z_i + \Delta Z_j$  in m.

#### Computation of Variables from Temperature Data

1. Note altitude of CAT occurrence ( $Z_{\text{CAT}}$ ). If a range is given compute mid-point as  $Z_{\text{CAT}}$  reference level.

2. Determine  $\frac{\Delta T}{\Delta Z}$  (in deg °C/100 m) for the sounding layer which includes the CAT level.

$$\frac{\Delta T}{\Delta Z} = \frac{100(T_{i+1} - T_i)}{Z_{i+1} - Z_i}$$

3. Extract all Z, T values within the region  $Z_{\text{CAT}} \pm 2000$  m. Compute  $\Delta T/\Delta Z$  for each layer within  $\pm 2000$  m of  $Z_{\text{CAT}}$ .

For  $\frac{\Delta T}{\Delta Z}$ ,  $(\frac{\Delta T}{\Delta Z})_{\text{max}}$  and  $(\frac{\Delta T}{\Delta Z})_{\text{min}}$ , determine the thickness  $\Delta Z$  and altitude  $\bar{h}$  of the center of the layer from which computation was made. It should be noted that  $(\frac{\Delta T}{\Delta Z})_{\text{max}}$  or  $(\frac{\Delta T}{\Delta Z})_{\text{min}}$  may equal  $\frac{\Delta T}{\Delta Z}$ .

A measure of the variability of the lapse rate will be computed next.

$$\text{Define } \gamma = \frac{\Delta T}{\Delta Z}; \gamma_{\text{min}} = (\frac{\Delta T}{\Delta Z})_{\text{min}}; \gamma_{\text{max}} = (\frac{\Delta T}{\Delta Z})_{\text{max}}$$

4. Compute  $\gamma_{\text{max}} - \gamma_{\text{min}}$ .

5. Order computed  $\gamma$ 's and  $\bar{h}$ 's according to increasing  $\bar{h}$ , i.e.,  $\gamma_1 \bar{h}_1, \gamma_2 \bar{h}_2, \gamma_3 \bar{h}_3$  where  $\bar{h}_3 > \bar{h}_2 > \bar{h}_1$ .

6. Compute  $\frac{\Delta\gamma}{\Delta Z} = \frac{\gamma_3 - \gamma_2}{h_3 - h_2} \times 100$

$$\frac{\Delta\gamma}{\Delta Z} = \frac{\gamma_2 - \gamma_1}{h_2 - h_1} \times 100$$

where  $\frac{\Delta\gamma}{\Delta Z}$  is in  $^{\circ}\text{C} (100 \text{ m})^{-1}$  per 100 m.

Note: In each computation a determination must be made that  $\bar{h}_3 \neq \bar{h}_2$  or that  $\bar{h}_2 \neq \bar{h}_1$ .

#### Computation of Variables from Wind Data

(1) As before, if a single level of CAT occurrence is given, this is taken as the reference level  $Z_{\text{CAT}}$ . If two levels are given, the midpoint is used.

(2) Determine for the wind sounding layer including  $Z_{\text{CAT}}$ :

$$\frac{\Delta\text{WD}}{\Delta Z} = \frac{100(\text{WD}_{i+1} - \text{WD}_i)}{Z_{i+1} - Z_i} \quad \frac{\Delta\text{WS}}{\Delta Z} = \frac{100(\text{WS}_{i+1} - \text{WS}_i)}{Z_{i+1} - Z_i}$$

where  $\frac{\Delta\text{WD}}{\Delta Z}$  is in degrees per 100 m and

$$\frac{\Delta\text{WS}}{\Delta Z} \text{ is in } \text{m sec}^{-1} \text{ per } 100 \text{ m.}$$

In addition to the scalar vertical wind shear and the change in wind direction with height, the magnitude of the vertical vector wind shear is computed as follows.

(Anderson [23].)

$$\left(\frac{\Delta\vec{V}}{\Delta Z}\right)^2 = \left(\frac{\Delta\vec{V}_x}{\Delta Z}\right)^2 + \left(\frac{\Delta\vec{V}_y}{\Delta Z}\right)^2 = \frac{(u_{i+1} - u_i)^2 + (v_{i+1} - v_i)^2}{(Z_{i+1} - Z_i)^2}$$

$$\frac{\Delta\vec{V}}{\Delta Z} = \frac{(u_2 - u_1)^2 + (v_2 - v_1)^2}{Z_{i+1} - Z_i} \cdot 100$$

where  $\frac{\Delta\vec{V}}{\Delta Z}$  is in  $\text{m sec}^{-1}$  per 100 m,

$u = -\text{WS} \sin \text{WD}$  and  $v = -\text{WS} \cos \text{WD}$ .

(3) Determine the product  $\bar{V} \times \frac{\Delta \vec{V}}{\Delta Z}$  as:

$$\frac{(WS_{i+1} + WS_i)}{2} \times \frac{\Delta \vec{V}}{\Delta Z},$$

where  $\frac{\Delta \vec{V}}{\Delta Z}$  is expressed in  $m \text{ sec}^{-1}$  per 100 m.

(4) Minor requirements are to determine the sounding level reporting the highest wind speed and to extract all variables for printout.

The variables derived from the wind data

$$\frac{\Delta WD}{\Delta Z}, \frac{\Delta WS}{\Delta Z}, \frac{\Delta \vec{V}}{\Delta Z}, V \times \frac{\Delta \vec{V}}{\Delta Z} \text{ and } \bar{V}$$

will be computed for a layer above and a layer below the central  $Z_{CAT}$  layer, provided the upper or lower limit of the layer is within the search layer ( $\pm 2000$  m of  $Z_{CAT}$  level). The subscripts U and L will denote the upper and lower layers, respectively.

#### Computation of Richardson Number

Richardson Number (Ri) is computed according to the expression

$$Ri = \frac{\frac{g}{\theta} \frac{\Delta \theta}{\Delta Z}}{\left(\frac{\Delta \vec{V}}{\Delta Z}\right)^2} = \frac{\frac{9.76}{T + 273} \left[ \frac{\Delta T}{\Delta Z} + 0.0098 \right]}{\left(\frac{\Delta \vec{V}}{\Delta Z}\right)^2}$$

where  $\frac{\Delta T}{\Delta Z}$  is expressed in  $^{\circ}C/m$  and  $\frac{\Delta \vec{V}}{\Delta Z}$  in  $\text{sec}^{-1}$ , i.e., the values are 1/100 of those computed in previous sections. T in  $^{\circ}C$  will be taken as an average of the two temperatures used to determine  $\frac{\Delta T}{\Delta Z}$ .

Ri will be computed as follows:

- (1) From values for  $\frac{\Delta T}{\Delta Z}$  and  $\frac{\Delta \vec{V}}{\Delta Z}$  computed in the layer encompassing  $Z_{CAT}$ .
- (2) From  $\left(\frac{\Delta T}{\Delta Z}\right)_{\min}$  and  $\frac{\Delta \vec{V}}{\Delta Z}$ . Rimi is computed Richardson Number.
- (3) From  $\left(\frac{\Delta T}{\Delta Z}\right)_{\max}$  and  $\frac{\Delta \vec{V}}{\Delta Z}$ . Rima is computed Richardson Number.

In the computation of Rimi and Rima, the vector vertical wind shear  $\frac{\Delta \vec{V}}{\Delta Z}$  used is computed from the central layer unless the  $\left(\frac{\Delta T}{\Delta Z}\right)_{\min}$  or  $\left(\frac{\Delta T}{\Delta Z}\right)_{\max}$  is embedded within an upper or lower layer for which a  $(\Delta \vec{V}/\Delta Z)_U$  or  $(\Delta \vec{V}/\Delta Z)_L$  has been computed.



#### 4. Output

The data listed below is printed out for each sounding—CAT case in the approximate order given:

radiosonde station call letter

radiosonde station number

station latitude

station longitude

day, month, year

time

altitude (range) of CAT occurrence

day and hour of CAT occurrence

terrain type

CAT intensity

approximate distance from radiosonde station

approximate latitude of CAT occurrence

approximate longitude of CAT occurrence

[ Note: each item listed above is contained on input card type 1 ].

tropopause and level of maximum wind data; P, Z, T, WD, WS at all levels

$$\frac{\Delta T}{\Delta Z}, \bar{h}, \Delta Z$$

$(\frac{\Delta T}{\Delta Z})_{\min}, \bar{h}_{\min}, (\Delta Z)_{\min}$ , may be the same as first set.

$(\frac{\Delta T}{\Delta Z})_{\max}, \bar{h}_{\max}, (\Delta Z)_{\max}$ , may be the same as first set.

$$\gamma_{\max} - \gamma_{\min}, \frac{\Delta \gamma_U}{\Delta Z}, \frac{\Delta \gamma_L}{\Delta Z}$$

$$\frac{\Delta WD}{\Delta Z}, \frac{\Delta WS}{\Delta Z}, \frac{\Delta \vec{V}}{\Delta Z}, \langle \bar{V} \cdot \frac{\Delta \vec{V}}{\Delta Z} \rangle, \bar{V} \text{ for a central layer and an upper and lower,}$$

if available.

Ri, Rimi, Rima